Dual contributions of Xrp1 to genome integrity through the DNA damage response and cell competition

Chaitali Khan[1,3], Nasser M Rusan[2] and Nicholas E Baker[1,4,5]

1. Department of Genetics, Albert Einstein College of Medicine, 1300 Morris Park Avenue, Bronx, NY 10461, USA.
2. Cell and Developmental Biology Center, National Heart, Lung, and Blood Institute, National Institutes of Health, Bethesda, MD 20892, USA.
3. Present address: Cell and Developmental Biology Center, National Heart, Lung, and Blood Institute, National Institutes of Health, Bethesda, MD 20892, USA.
4. Present address: Department of Microbiology and Molecular Genetics, and Department of Developmental and Cell Biology, University of California, Irvine, CA 92697, USA.
5. Author for correspondence: nebaker@uci.edu

ABSTRACT

Model organisms may help understand how p53 suppresses tumorigenesis in mammals. In *Drosophila*, the primary transcriptional target of p53 is the gene encoding the bZip AT-hook protein Xrp1, which is another transcription factor. We report that Xrp1 mediated multiple functions of p53 in the DNA damage response (DDR), contributing to p53-dependent gene transcription and DNA damage-induced apoptosis. In addition to this role as a p53 effector, a p53-independent role for Xrp1 in cell competition has been described. Cell competition can remove cells whose genome has been altered by DNA damage and repair. During cell competition, Xrp1 is induced by RpS12, which acts as a sensor of defective ribosome biogenesis. RpS12-dependent cell competition began as the DDR wound down, and was even more prominent if p53 function was reduced. Such p53 inhibition resulted in persistence of DNA damage revealed by γH2Av accumulation. Thus, Xrp1 limited the accumulation of abnormal cells resulting from genotoxicity through both the acute, p53-dependent DDR, and also from subsequent cell competition that removes cells where DNA repair did not restore the normal genome. Both these processes might contribute to the tumor suppressor function of p53 in mammals.

INTRODUCTION

Maintaining genome integrity is essential not only to preserve genetic information in the germline but also for somatic cells. Defects in DNA repair are associated with elevated cancer incidences, and defects in mitotic fidelity occur in aging (Tiwari & Wilson, 2019; Vijg, 2021; Hopkins et al., 2022; Nemeth & Szuts, 2024). Most cancer cells are aneuploid, and both mouse models and human genetic diseases that predispose to aneuploidy are cancer prone (Hanks et al., 2004; Baker et al., 2009; Baker & van Deursen, 2010). The most important human tumor suppressor, p53, is well known as a master regulator of the DNA damage response (DDR) that also maintains the integrity of somatic tissues by the apoptotic elimination of cells with damaged DNA (Levine et al., 2006; Zhang et al., 2011). P53 also has other functions, and it has been questioned whether the DNA damage response is, in fact, responsible for its tumor suppressor function (Kaiser & Attardi, 2018; Boutelle & Attardi, 2021). In addition to apoptosis as a cell-autonomous response to DNA damage, a process of cell competition has also been described in which damaged cells can be removed only when they are less fit than their neighbors (Baker, 2020; Baker & Montagna, 2022; Kiparaki & Baker, 2023; Khandekar & Ellis, 2024; Nagata & Igaki, 2024). Cell competition is able to remove cells with damage that would be tolerated by cell-autonomous mechanisms. In *Drosophila*, cell competition occurs independently of p53 (Kale et al., 2015), but in mammals, p53 activities too low to cause apoptosis by cell-autonomous mechanisms can trigger competitive cell removal when compared with less affected surrounding cells (Bondar & Medzhitov, 2010a; Wagstaff et al., 2016; Zhang et al., 2017; Fernandez-Antoran et al., 2019).

In *Drosophila*, the *Xrp1* gene is a common link between the DNA damage response and cell competition. Xrp1 was first described as a transcriptional target of p53, encodes a *Drosophila* bZip domain protein, and is transcriptionally induced by p53 when *Drosophila* embryos are irradiated (Brodsky et al., 2004; Akdemir et al., 2007). Flies lacking wild-type Xrp1 exhibit increased sensitivity to irradiation. Specifically, they show increased loss of heterozygosity in an assay that quantifies patches of cells expressing the recessive *mwh* phenotype in otherwise $mwh^{+/-}$ individuals, indicative of somatic loss of the mwh^{+} allele (Akdemir et al., 2007). This loss of heterozygosity following irradiation is consistent with a role for Xrp1 in the DDR, regulated by p53.

Xrp1 was later identified as a central regulator of the cell competition of 'Minute' (Ribosome protein gene heterozygous mutant) cells in imaginal discs (Lee et al., 2016; Baillon et al., 2018; Lee et al., 2018b; Brown et al., 2021). Cell competition was first described as a phenomenon affecting cells heterozygous for mutations in genes encoding Ribosomal proteins (Rp) (Morata & Ripoll, 1975). Most Rp genes are essential, so *Rp* mutations are generally homozygously lethal, whereas $Rp^{+/-}$ heterozygotes survive with a developmental delay, thin bristles, and some other traits (Bridges & Morgan, 1923; Marygold et al., 2007). In contrast to whole $Rp^{+/-}$ animals, individual $Rp^{+/-}$ cells or clones are eliminated from many tissues when wild-type cells are also present, suffering an enhanced rate of apoptosis (Morata & Ripoll, 1975; Simpson, 1979; Moreno et al., 2002; Li & Baker, 2007). The Xrp1 protein is expressed at only low levels in wild-type imaginal discs, but Xrp1 protein is robustly induced in $Rp^{+/-}$ cells, where it is required for transcriptional changes in $Rp^{+/-}$ wing discs and for many aspects of the $Rp^{+/-}$ phenotype, including both developmental delay and cell competition (Baillon et al., 2018; Lee et al., 2018b; Boulan et al., 2019). Xrp1 binds to DNA as a heterodimer with another protein, Irbp18. Unlike Xrp1, Irbp18 is abundantly expressed in wild-type imaginal disc cells (Reinke et al., 2013; Francis et al., 2016; Blanco et al., 2020). The Xrp1/Irbp18 heterodimer activates transcription by binding to a sequence motif identified from both in vitro studies and ChIP-Seq *in vivo* (Zhu et al., 2011; Baillon et al., 2018; Kiparaki et al., 2022). Like Xrp1, Irbp18 is also required for cell competition, suggesting that transcriptional targets of the Xrp1/Irbp18 heterodimer are involved (Blanco et al., 2020).

Unlike Xrp1 expression following irradiation, Xrp1 induction in $Rp^{+/-}$ cells does not require p53, and p53 is also not needed for the competitive elimination of $Rp^{+/-}$ cells from mosaics (Kale et al., 2015; Lee et al., 2018b). In $Rp^{+/-}$ cells, Xrp1 expression is induced by a particular Rp, RpS12, which is necessary for cell competition (Kale et al., 2018; Lee et al., 2018b; Ji et al., 2019). Mutations in other *Rp* genes, and other ribosome biogenesis defects such as diminished rRNA synthesis, behave as though they increase RpS12 function (Baker & Kale, 2016; Ji et al., 2019; Kiparaki et al., 2022). RpS12 activates Xrp1 expression through alternative splicing of the Xrp1 mRNA (Kakemura et al., 2025; Potiri et al., 2025). Other cellular stresses can also activate Xrp1 expression, at least some independently of both p53 and RpS12 (Baumgartner et al., 2021; Brown et al., 2021; Ochi

105 et al., 2021; Recasens-Alvarez et al., 2021; Kiparaki et al., 2022; Kumar & Baker, 2022;
106 Kiparaki & Baker, 2023; Shekhar et al., 2025).

107 In *Drosophila*, cell competition is part of the response to aneuploidy(Titen & Golic,
108 2008; McNamee & Brodsky, 2009; Ji et al., 2021a; Baker & Montagna, 2022). Because
109 the genes encoding 80 Rp are distributed around the chromosomes, loss of chromosome
110 segments constituting more than 1.2% of the genome (on average) typically leads to
111 haploinsufficiency for one *Rp* gene or another by removing one copy of that locus. This
112 leads to the elimination of cells bearing many segmental monosomies by the same cell
113 competition pathway that affects $Rp^{+/-}$ point mutant cells (Ji et al., 2021b). Accordingly,
114 *Drosophila* lacking cell competition can accumulate cells with certain kinds of genetic
115 damage, not because they experience any defect in DNA repair, but because some
116 abnormal genotypes that would ordinarily be eliminated by cell competition survive when
117 cell competition is inhibited. Adult flies with a mutation in RpS12 that prevents cell
118 competition exhibit an increased frequency of sporadic cells exhibiting the typical $Rp^{+/-}$
119 mutant thin bristle phenotype, whether occurring spontaneously or after irradiation. Many
120 of these cells likely harbor chromosome deletions that affect multiple genes in addition to
121 one of the *Rp* loci (Ji et al., 2021b).

122 Because Xrp1 has been implicated in two processes that impact genome integrity,
123 we sought here to define the respective roles more precisely. Loss of heterozygosity after
124 irradiation of Xrp1 mutants could either arise through defects in p53-dependent DNA
125 repair or apoptosis, or due to failure to outcompete cells bearing irradiation-induced
126 segmental aneuploidies. We now report that Xrp1 is indeed important for the DDR as well
127 as for cell competition, mediating the expression of most of the p53-target genes and
128 contributing to p53-induced apoptosis and the repair or removal of DNA damage. If cells
129 with unrepaired DNA and damaged genomes accumulate after DNA repair, many of these
130 are subsequently removed by p53-independent, Xrp1-dependent cell competition. Thus,
131 Xrp1 plays at least two temporally distinct roles in genome integrity.

132 These findings may provide insight into mammalian cancer development. P53 is
133 one of the most important human tumor suppressors, mutated in more than 50% of human
134 cancers (Muller & Vousden, 2014). Although p53 ensures genomic integrity as the key
135 effector of the DDR (Levine et al., 2006; Kastenhuber & Lowe, 2017), it has been

136 questioned whether this is the basis for tumor suppression. Point mutations that block
137 p53 function in the acute DDR have little effect in blocking tumor growth, and conditional
138 knock-out studies point to a critical window for tumor suppressor function that is
139 subsequent to the resolution of DNA damage (Christophorou et al., 2005; Christophorou
140 et al., 2006; Li et al., 2012; Kaiser & Attardi, 2018). In mammals, which seem to lack a
141 clear Xrp1 ortholog, p53 is required for cell competition, potentially substituting
142 functionally for the role of Xrp1 in *Drosophila* (Baker et al., 2019; Baker, 2020; Lacroix et
143 al., 2020; Boutelle & Attardi, 2021; Pilley et al., 2021). Cell competition could provide a
144 second role for mammalian p53 in genome integrity, contributing to tumor suppression,
145 for example, if it were found to eliminate aneuploid cells, analogous to the way that Xrp1
146 contributes to both DDR and cell competition in *Drosophila*.
147
148 RESULTS
149 **DNA damage-induced expression of Xrp1**
150 Studies on irradiated *Drosophila* embryos and larval tissues indicate that DNA Damage-
151 induced apoptosis proceeds in two distinct phases (Wells et al., 2006; Wichmann et al.,
152 2006; McNamee & Brodsky, 2009; Ji et al., 2021a). An initial acute, p53-dependent DDR
153 peaks in the first 4 hours (Figure 1A). This is followed by a later, p53-independent phase
154 that is associated with cell competition (Figure 1A). Xrp1 mRNA is upregulated by p53
155 within 30 minutes of irradiation of *Drosophila* embryos (Brodsky et al., 2004; Akdemir et
156 al., 2007), perhaps by direct binding of p53 within the Xrp1 locus (Kurtz et al., 2019). We
157 explored Xrp1 mRNA and protein expression to confirm that Xrp1 is a p53 target in third-
158 instar larval wing discs. We used a fly line in which the Xrp1 protein was expressed from
159 the endogenous locus, containing a C-terminal HA tag (Blanco et al., 2020). Wild-type
160 wing discs exhibited only a few Xrp1-HA-positive cells, possibly reflecting spontaneous
161 DNA damage or other cellular stress (Figure 1B). Exposure to ionizing radiation (IR: 1500
162 Rads of γ-rays) induced strongly Xrp1-HA positive cells by 2 hours after IR, which further
163 increased by 4 hours after IR (Figure 1C-D). The DNA damage-induced Xrp1-HA
164 expression was non-uniform, with some cells showing higher expression levels than
165 others. This heterogeneity was different from the more uniform Xrp1-HA expression seen
166 in $Rp^{+/-}$ mutant wing discs (Figure 1E). A similar salt-and-pepper pattern of Xrp1 was

observed with the Xrp1 antibody (Figure 1F, G). The specificity of Xrp1-HA expression was further confirmed by its reduction after RNAi for Xrp1 (Figure 1H).

We tested the requirement of p53 using a dominant-negative form encoded by the *UAS-p53*^{H159N} transgene. We drove expression in posterior wing compartments so that Xrp1-HA expression levels could be compared to the anterior compartments of the same wing discs as a control. Dominant-negative p53 significantly reduced IR-induced Xrp1-HA (Figure 1I). Xrp1 in imaginal disc was also p53-dependent at the transcript level, with a ~3x reduction in mRNA level seen after qRT-PCR from irradiated *p53*$^{-/-}$ wing discs (Figure 1- figure supplement 1A).

Interestingly, IR-induced Xrp1-HA protein expression was only slightly affected by Irbp18 knockdown (Figure 1J). This was different from Xrp1 expression in *Rp*$^{+/-}$ mutants, where Xrp1 autoregulation is important to regulate the level of Xrp1 expression (Baillon et al., 2018; Blanco et al., 2020). Consistent with autoregulation not contributing to IR-induced *Xrp1* transcription, 50% of the normal *Xrp1* mRNA level remained in the *Xrp1*$^{m2-73}$*/Df* mutant background (Figure 1- figure supplement 1A). Thus, the *Xrp1*$^{m2-73}$ point mutant allele could still be transcribed in response to irradiation, even without a functional Xrp1 product.

An Xrp1-LacZ enhancer trap has also been used as a reporter previously. It is upregulated in *Rp*$^{+/-}$ mutant wing discs (Baillon et al., 2018; Lee et al., 2018a). Like Xrp1 protein and mRNA, Xrp1-LacZ was moderately elevated after irradiation (Figure 1K,L). Different from Xrp1-HA, Xrp1-LacZ expression depended on Xrp1 and Irbp18 function, both after irradiation and in the unirradiated control (Figure 1- figure supplement 1B-E). Unexpectedly, reducing p53 function slightly elevated the expression of Xrp1-LacZ after irradiation (Figure 1M). These differences might be explained if there is an autoregulatory component to Xrp1 transcription, particularly affecting Xrp1-LacZ, that does not contribute much to IR-induced Xrp1 mRNA or protein levels.

Regulation of p53-dependent DDR target genes by Xrp1

In mammals, p53 regulates a complex transcriptional program of hundreds or even thousands of genes (Levine et al., 2006). Depending on the study, however, only 122-346 p53-dependent genes have a p53 consensus motif in the promoter or upstream

198 region (Wei et al., 2006; Fischer, 2017). It is thought that p53 directly controls core
199 transcription programs that, in turn, regulate further secondary, indirect targets (Andrysik
200 et al., 2017). Xrp1 is a candidate for bringing secondary target genes under the indirect
201 control of *Drosophila* p53. Consistent with this, when we compared 42 rapidly induced
202 p53-target genes (RIPD) identified in the DDR (Brodsky et al., 2004; Akdemir et al., 2007),
203 with Xrp1-dependent genes expressed in $Rp^{+/-}$ wing imaginal discs or discs
204 overexpressing Xrp1 (Baillon et al., 2018; Lee et al., 2018b), we found 21 of 42
205 overlapped (Figure 2A). These genes were associated with Gene Ontology (GO) terms
206 transcription factors, cell death, DNA repair, and redox response (Figure 2B).

207 To test if Xrp1 was needed to express p53-dependent genes in response to IR, we
208 employed available reporter lines and also confirmed gene expression by qRT-PCR.
209 *GstD-lacZ* is a redox response reporter that is induced in response to oxidative stress
210 (Sykiotis & Bohmann, 2008; Brown et al., 2021) and is elevated by Xrp1 in $Rp^{+/-}$ wing
211 discs (Kucinski et al., 2017; Ji et al., 2019; Kiparaki et al., 2022). *GstD-lacZ* was
212 expressed in response to IR, dependent on p53 (Figure 2C-D). We found that Xrp1 and
213 Irbp18 were needed (Figure 2F-G). This was in accordance with Xrp1/Irbp18 binding sites
214 being present in the *GstD*-lacZ reporter (Brown et al., 2021). To confirm that antioxidant
215 genes themselves were affected like the *GstD-lacZ* reporter was, we measured *GstD1*
216 mRNA levels in wing discs. Induction of *GstD1* mRNA by IR indeed depended on both
217 p53 and Xrp1 (Figure 2M).

218 Another stress pathway activated in DDR is the Jun N-terminal Kinase (JNK)
219 pathway (Picco & Pages, 2013). JNK activity is also Xrp1-dependent in $Rp^{+/-}$ wing discs
220 (Lee et al., 2018b; Ji et al., 2019). We found the JNK reporter *TRE-dsRed* was induced
221 by IR in a p53-dependent manner (Figure 2H-J), and this was Xrp1/Irbp18 dependent
222 (Figure 2K & L). The TNF-alpha ligand *eiger (egr)* has been proposed to activate JNK
223 signaling in the DDR (Sanchez et al., 2019). Surprisingly, however, *egr* transcription was
224 p53-dependent but independent of Xrp1, which questions whether it is solely responsible
225 for JNK signaling in the DDR (Fig. 2N).

226 All except one of the p53-dependent DNA repair genes induced in DDR were also
227 potential Xrp1 targets (Figure 2B). We measured wing disc mRNA levels of representative
228 genes from the major DNA repair pathways. These were the homologous recombination

229 pathway gene *rad50*, the translesion polymerase DNA polymerase zeta subunit 1,
230 *mus205*, and the Non-Homologous End Joining (NHEJ) pathway genes DNA ligase 4
231 (*lig4*) and *Ku80*. We found that IR-dependent expression of all these genes depended on
232 Xrp1 at least as strongly as upon p53 (Figure 2O-R).

233 A well-known aspect of DDR is the apoptotic death of severely damaged cells,
234 dependent in *Drosophila* on p53-dependent induction of the pro-apoptotic genes *rpr* and
235 *hid* (Brodsky et al., 2004; Dekanty et al., 2015). To explore the potential role of Xrp1, we
236 examined reporter lines for *rpr* and *hid*, which are expressed in response to IR and are
237 widely used as p53 reporters (Brodsky et al., 2004; Tanaka-Matakatsu et al., 2009; Fan
238 et al., 2010). Two reporter lines for *hid* are the *hid5'F-wt-EGFP* reporter, which contains
239 ~2 kb spanning the *hid* promoter from +16 to −2210bp relative to the transcription start
240 site, and the $hid^{20\text{-}10}$-*lacZ* reporter, which includes a distinct 10 kb sequence from the *hid*
241 upstream region (Tanaka-Matakatsu et al., 2009; Fan et al., 2010) (Figure 3A). As
242 expected, *hid5'F-wt-EGFP* was highly induced after IR in a p53-dependent manner
243 (Figure 3B-D). Both *Xrp1* RNAi and *Irbp18* RNAi reduced the *hid5'F-wt-EGFP* expression
244 to the same extent as p53 dominant-negative did (Figure 3E-F). The $hid^{20\text{-}10}$-*lacZ* reporter
245 was also induced by IR and was dependent upon p53 (Figure 3G-I). Both *Xrp1* and *Irbp18*
246 RNAi reduced IR-dependent $hid^{20\text{-}10}$-*lacZ* expression, although not so much as p53
247 dominant-negative (Figure 3J-K). We assessed *rpr* expression using the rpr^{150}-*lacZ*
248 reporter, containing a 150bp sequence including a putative p53 binding site ~4.8kb
249 upstream of the *rpr* gene (Brodsky et al., 2000). In controls, rpr^{150}-*lacZ* reporter exhibits
250 uniform expression in most of the wing disc, on which is superimposed a region of
251 elevated expression bordering the posterior wing pouch and notum region (Alpar et al.,
252 2018; Li et al., 2020) (Figure 3L). It is now appreciated that many DDR genes have non-
253 uniform expression patterns in the wing disc (Cruz et al., 2025). Because IR enhanced all
254 aspects of rpr^{150}-*lacZ* expression (Figure 3L, M, and Figure 3- figure supplement 1A), we
255 measured the average rpr^{150}-*lacZ* expression level in anterior and posterior
256 compartments and computed the ratio of posterior-to-anterior expression level as a
257 readout of genetic perturbations applied to the posterior compartments (Figure 3- figure
258 supplement 1B). The increase in rpr^{150}-*lacZ* following IR was p53-dependent, as

259 expected, but unaffected by RNAi for either Xrp1 or Irbp18 (Figure 3N-P- figure
260 supplement 1B).
261 To confirm that these studies of *hid* and *rpr* reporters were indeed reflective of the
262 expression of the genes themselves, mRNA levels were measured in wing discs after IR.
263 Consistent with the reporter studies, induction of *hid* mRNA by irradiation was completely
264 dependent on p53 and partially dependent on Xrp1 (Figure 3Q). Induction of *rpr* mRNA
265 expression was completely dependent on p53 but was unaffected by the loss of Xrp1
266 (Figure 3R).
267 Taken together, these results show that genes identified as p53 targets in the
268 *Drosophila* DDR include genes that are, in fact, directly induced by Xrp1. Only two out of
269 nine p53 target genes examined, *egr* and *rpr*, were induced independently of Xrp1,
270 although *hid* induction has both Xrp1-dependent and -independent components. Analysis
271 of p53 and Xrp1 binding motifs supported this conclusion. Sequences matching the p53
272 binding consensus have been located within both the rpr^{150}*-lacZ* reporter and the *hid5'F-*
273 *wt-EGFP* reporter (Brodsky et al., 2000; Wichmann et al., 2010). Consensus binding sites
274 for the Xrp1/Irbp18 heterodimer have been determined by bacterial one-hybrid studies
275 (Fly Factor Survey) (Zhu et al., 2011) and from ChIP-seq after Xrp1 overexpression in
276 wing disc (Baillon et al., 2018). Such sequences are footprinted by Xrp1/Irbp18 in the P
277 element terminal repeat (Francis et al., 2016) and are sufficient to confer Xrp1/Irbp18-
278 dependent transcription on luciferase reporters (Kiparaki et al., 2022). Using an *in-silico*
279 motif finder (INSECT) (Rohr et al., 2013), we found two Xrp1/Irbp18 binding motifs in the
280 *hid5'F-wt-EGFP* reporter sequence and two in the $hid^{20\text{-}10}$*-lacZ* reporter sequence (Figure
281 3T), but we found none in the rpr^{150}*-lacZ* reporter that was expressed independently of
282 Xrp1 and Irbp18 (Figure 3T). We conclude that, while *rpr* could be a direct target of p53
283 in the DDR, *hid* expression is partially dependent on Xrp1 induction downstream of p53,
284 and the *hid5'F-wt-EGFP* reporter entirely so.
285
286 **Xrp1 is sufficient for the expression of p53-dependent DDR target genes**
287 It was possible that the only Xrp1 requirement in the DDR might be to activate p53
288 to create a positive feedback loop. We used the rpr^{150}*-lacZ* reporter, which is activated by
289 p53 but not Xrp1, to test how p53 activity was affected by Xrp1 overexpression. Xrp1

290 overexpression in the wing pouch resulted in a huge amount of cell death, as expected
291 (Figure 4- figure supplement 1A-B), but no discernible increase in *rpr*^{150}*-lacZ* levels
292 (Figure 4- figure supplement 1C-D). Similar results were obtained by expressing Xrp1 in
293 the eye discs (Fig. 4A-B). Thus, Xrp1 did not cause p53 activation and is likely to act
294 downstream of p53.

295 Next, we tested if Xrp1 was sufficient for the expression of target genes. Xrp1
296 overexpression in the eye disc led to a robust upregulation of *hid*$^{20\text{-}10}$*-lacZ* (Figure 4C and
297 D) and *hid5'F-wt-EGFP* (Figure 4E and F). Xrp1 also regulated JNK and *GstD* after DNA
298 damage, and Xrp1 overexpression was sufficient to activate the reporters for these
299 pathways, *TRE-dsRED* and *GstD-lacZ* (Figure 4- figure supplement 1E and F & G and
300 H). These results show that Xrp1 functions downstream of p53 and is sufficient for
301 expressing a subset of p53-dependent DDR genes.
302

303 **Xrp1 contributes to DNA damage-induced cell death**

304 To see whether the regulation of cell death genes by Xrp1 was functionally
305 significant, the *p53*-dependent apoptosis that occurs in response to irradiation was
306 examined. Cell death begins within 30 minutes after IR treatment and is entirely
307 dependent on p53 for at least 4-5 hours (Wichmann et al., 2006; McNamee & Brodsky,
308 2009). Accordingly, p53 dominant-negative expression in posterior compartments
309 substantially reduced the IR-induced cell death, leaving only a few cells positive for the
310 activated Dcp-1 caspase (Figure 5A, B, D). Xrp1 RNAi (two independent lines) and Irbp18
311 RNAi both reduced cell death in the posterior compartment (Figure 5C, D) to a lesser
312 extent than p53 dominant-negative did.

313 We also examined the cell autonomy of p53 and Xrp1 function using clones of
314 mutant cells. Control clones did not affect IR-induced cell death (Figure 5E, H). Wild-type
315 and *p53*$^{+/-}$ heterozygous cells exhibited similar cell death levels after irradiation, but cell
316 death was absent from *p53*$^{-/-}$ null clones (Figure 5F, H). There was little cell death
317 observed in *Xrp1*$^{+/-}$ (heterozygous) and *Xrp1*$^{-/-}$ (null) tissue as opposed to the high amount
318 of cell death observed in *Xrp1*$^{+/+}$ (wild type twin spot) (Figure 5G, H) (effects of Xrp1
319 mutation on *Rp* mutant cells are also dominant through haploinsufficiency) (Lee et al.,
320 2018b). Taken together, these results show that Xrp1 contributes to p53-mediated cell

321 death in response to irradiation, although this is partial because p53 also regulates cell
322 death genes directly, such as *rpr* (Figure 3R).
323 We also tested the contribution of Xrp1 to the effects of p53 overexpression. Over-
324 expression of p53 in the developing eye causes a rough eye phenotype in adults (Figure
325 5- figure supplement 1A) (Jin et al., 2000; Ollmann et al., 2000). Xrp1 knockdown very
326 slightly reduced the rough eye phenotype, unlike dominant-negative p53, which rescued
327 completely (Figure 5- figure supplement 1B, C). p53 overexpression in wing discs resulted
328 in massive cell death that was reduced only weakly by Xrp1 knockdown or mutant
329 genotypes (Figure 5- figure supplement 1D-H). In accordance with this partial
330 dependence on Xrp1, p53 overexpression led to rather little Xrp1 protein expression
331 (Figure 5- figure supplement 1I). These differences suggest that the effects of p53
332 overexpression differ from endogenous p53 activity in the physiological DDR, which
333 depends on Xrp1 to a considerable degree.
334
335 **Xrp1-dependent competitive cell death limits genomic instability**
336 The DDR is followed by a phase of p53-independent cell death, peaking around
337 24h after irradiation, reflecting the loss of aneuploid cells (Wichmann et al., 2006;
338 McNamee & Brodsky, 2009). We previously showed that the majority of this p53-
339 independent cell death depends on RpS12 and is associated with the expression of Xrp1,
340 consistent with cell competition on the basis of altered *Rp* gene dose (Ji et al., 2021b).
341 Here, we confirmed that most of the p53-independent cell death depends on Xrp1 (Figure
342 6A-F). At 24 hours after irradiation, Xrp1-HA expression was still observed and was totally
343 suppressed upon Xrp1 knockdown (Figure 6- figure supplement 1A-C). Irbp18
344 knockdown reduced Xrp1-HA expression to some extent in accordance with the
345 autoregulatory role of Irbp18/Xrp1 in cell competition (Figure 6- figure supplement 1D, G).
346 It was already known that Xrp1 expression at this stage did not require p53 (Ji et al.,
347 2021a); surprisingly, Xrp1-HA expression was actually increased when p53 was inhibited
348 (Figure 6- figure supplement 1E, G). This increase was reduced in the *rpS12* mutant
349 (Figure 6- figure supplement 1F, G). Importantly, in addition to not affecting cell death at
350 2 hours after IR (Figure 6- figure supplement 1H, I) (Ji et al., 2021a), RpS12 also does
351 not affect Xrp1-HA expression at 2 hours after IR (Figure 6- figure supplement 1J-L).

352 Thus, Xrp1 expression and function in the acute DDR depended on p53, not RpS12. In
353 contrast, the Xrp1 expression that occured 24 hours after irradiation depended at least in
354 part on RpS12, as did the enhanced expression that occured in the absence of p53.

355 To explore the impacts of p53 on genome integrity and Xrp1 activity further, we
356 looked at IR-induced DNA damage using antibodies against γH2Av, which marks the
357 double-strand breaks (Lake et al., 2013; Khan et al., 2017). Consistent with previous
358 reports, most of the acute DNA damage visible 4h after irradiation was repaired by 24
359 hours (Figure 6A-C) (Wells et al., 2006; McNamee & Brodsky, 2009). Like Xrp1-HA
360 expression, γH2Av levels 24 hours after irradiation were increased in the absence of p53,
361 indicating persistent unrepaired DNA damage (Figure 6D). Dual Xrp1 knockdown and p53
362 inhibition led to an even further increase (Figure 6E). These data indicated that p53 was
363 required for the repair (or removal) of irradiation-damaged DNA, and that some cells
364 where this damage persists were then removed by p53-independent Xrp1 activity, i.e.,
365 cell competition. Consistent with this conclusion, double labeling showed that some of the
366 γH2Av-positive cells that persisted when p53 was inhibited also expressed Xrp1-HA
367 (Figure 6G-H). In support of the p53-independent function of Xrp1 at 24 hours post-IR,
368 the expression of *hid5'F-wt-EGFP* was totally dependent on Xrp1 at this stage, but not all
369 this expression depended on p53 (Figure 6J, I). However, we noticed that a fraction of
370 *hid5'F-wt-EGFP* expression at 24 hours post-IR was still p53-depedent but to a much
371 lesser extent that at 4 hours (Figure 3).

372 To get a better idea of when cell competition begins, wing discs were examined 16
373 hours post-IR. We found that Xrp1-HA expression was largely independent of p53 by 16
374 hours (Figure 6- figure supplement 2A-C) and, in fact, similar to 24 hours, Xrp1 was
375 elevated in the absence of p53. However, similar to 4 hours after IR, Xrp1 knockdown
376 completed suppressed Xrp1-HA expression at 16 hours post-IR but Irpb18 did not (Figure
377 6- figure supplement 2D, E). Cell death occurring 16 hours after irradiation was
378 substantially p53-dependent, but p53-independent cell death was also detected (Figure
379 6- figure supplement 2F, G & I), in contrast to the acute DDR phase, where cell death is
380 almost completely p53 dependent (Figure 5). Cell death 16 hours following irradiation was
381 reduced by Xrp1 and Irbp18 depletion, but not eliminated (Figure 6- figure supplement
382 2F, H & I). These results suggest that p53-independent Xrp1 expression and function in

383 cell competition are emerging by 16 hours and peaking by 24 hours after irradiation,
384 perhaps indicating the timeline of the appearance of aneuploid cells.
385
386 DISCUSSION
387 Xrp1 is known to contribute to genome integrity because flies lacking Xrp1 exhibit
388 increased loss-of-heterozygosity following irradiation (Akdemir et al., 2007; Ji et al.,
389 2021b). Here, we affirm that Xrp1 contributes to genome maintenance at two levels
390 (Figure 7). One is as a component of the acute DDR, mediating part of the p53
391 transcriptional response and p53-dependent apoptosis; the other role occurs later,
392 through cell competition to eliminate aneuploid and segmentally aneuploid cells that have
393 acquired altered Rp gene dose as a result of DNA damage and its subsequent repair
394 (Figure 7A). Xrp1 expression is induced by p53 in the DDR and by RpS12 during cell
395 competition. Defects in the DDR, eg, when p53 is inhibited, increase the aneuploid cell
396 burden and the resulting need for cell competition (Figure 7B,C). These two processes
397 are distinguished in *Drosophila* by the distinct roles of p53 and of RpS12 in Xrp1 induction
398 in each case. In mammals, however, both the DDR and cell competition depend on p53
399 and are both potential contributors to p53-mediated tumor suppression.
400
401 **Xrp1 is an effector of p53 functions in the DDR**
402 In imaginal discs, Xrp1 is induced by p53 activity in the acute phase of DDR at
403 both RNA and protein levels (Figure 1). Unlike Xrp1 induction in $Rp^{+/-}$ cells, Xrp1
404 expression in the DDR occurs independently of autoregulatory transcription, which may
405 be why the Xrp1-LacZ enhancer trap shows less upregulation than the endogenous Xrp1
406 transcript and protein. Multiple p53-dependent DDR genes, in fact, the majority in our
407 study, were Xrp1-dependent, including the pro-apoptotic gene *hid*. Even though *hid*-
408 reporters have been used as readouts of p53 activity (Fan et al., 2010; Zhang et al., 2014;
409 Chakravarti et al., 2022; Ruiz-Losada et al., 2022), they may be more accurately
410 described as targets of Xrp1. Other Xrp1 targets in the DDR include DNA repair genes,
411 GstD1, and JNK signaling. Accordingly, Xrp1 is functionally required in the DDR. DNA
412 damage-induced cell death is reduced in the absence of Xrp1, although not eliminated,
413 perhaps because the pro-apoptotic gene *rpr* seems to be a direct target of p53, whose

414 transcriptional induction does not require Xrp1. The absence of Xrp1 also leads to an
415 increase in persistent DNA damage, as evidenced by persistent γH2Av staining. This is
416 even more pronounced when p53 is absent as well (Figure 6). Persistent γH2Av staining
417 may reflect ineffective DNA repair, insufficient apoptosis that permits badly damaged cells
418 to survive, or both.
419 We show that in *Drosophila*, Xrp1 acts downstream to p53 as an intermediate
420 transcription factor and probably controls the majority of DDR targets. So far, integrating
421 data from gene expression studies, binding motif and ChIP-Seq searches, and global run-
422 on sequencing of nascent mRNA has not yielded a consensus on the core set of direct
423 p53 target genes in mammals (Riley et al., 2008; Allen et al., 2014; Fischer, 2017). It is
424 possible that, as in *Drosophila*, mammalian p53 acts as a master transcription factor that
425 regulates a network of gene expression responses both directly and through intermediate
426 transcription factors.
427
428 **Xrp1 acts independently of p53 in cell competition**
429 Although Xrp1 protein expression was almost completely p53-dependent during
430 the acute DDR response, later Xrp1 expression was mostly p53-independent (Figure 6-
431 figure supplement 1). Most DNA damage is normally resolved by the time of p53-
432 independent Xrp1 expression (Wells et al., 2006). Without p53, however, DNA damage
433 persisted longer than usual, so γH2Av labeling was still evident 24h after irradiation
434 (Figure 6).
435 Previous work shows that p53-independent cell death can reflect cell competition
436 of cells whose genomes have been altered by irradiation. Because 80 Rp are encoded
437 by genes spread throughout the genome, a loss of 1-2% of the genome will often create
438 haploinsufficiency for one or more Rp genes and trigger elimination by cell competition
439 (Ji et al., 2021b). Consistent with this mechanism, the delayed, p53-independent Xrp1
440 expression largely depended on RpS12, a signal of defective ribosome biogenesis that is
441 required to induce Xrp1 expression in $Rp^{+/-}$ cells and cells with defective rRNA synthesis
442 (Lee et al., 2018b; Kiparaki et al., 2022). Accordingly, the p53-independent apoptosis
443 occurring 24 hours after IR, and which is known to depend on RpS12, also depended on
444 Xrp1. Xrp1 thus contributes to genome integrity at two levels, as a component of the p53-

445 dependent DDR and as an executor of RpS12-dependent cell competition that functions,
446 in part, to remove cells where DDR has failed or has altered cell genotypes (Figure 7B,C).
447 Notably, Xrp1 expression levels were several-fold higher during the cell
448 competition phase if p53 had been inhibited (Figure 6- figure supplement 1). Because this
449 expression is p53-independent and likely to represent cell competition of aneuploid cells,
450 it suggests that more aneuploid cells arise without p53 to coordinate the DDR. The
451 persistence of H2Av labeling also suggested that double-strand breaks persist without
452 p53. We think that without p53, DNA repair pathways, including DSB repair, single-strand
453 break repair, and Nucleotide excision repair, are delayed or less effective, and coupled
454 with faulty cell cycle arrest, result in a higher frequency of genome rearrangements and
455 aneuploidy (Williams & Schumacher, 2016).
456
457 **Dual processes maintaining genome integrity following DNA damage**
458 We have focused on two Xrp1-dependent processes contributing to genome
459 integrity after DNA damage. The DDR depends on p53 in both *Drosophila* and mammals.
460 Cell competition removes aneuploid cells in a p53-independent manner in *Drosophila*
461 (Figure 7).
462 In mammals, the DDR was initially thought to represent the tumor suppressor
463 function of p53. Later studies showed that tumor suppression is separable from the DDR
464 and occurs afterwards (Christophorou et al., 2005; Christophorou et al., 2006; Li et al.,
465 2012; Kaiser & Attardi, 2018). In mammals, where no clear Xrp1 homolog exists, Rp
466 gene haploinsufficiency instead induces p53 through the nucleolar stress pathway
467 (Bursac et al., 2014). Interestingly, differences in p53 activity levels between cells underlie
468 multiple examples of cell competition in mammals (Bondar & Medzhitov, 2010b; Marusyk
469 et al., 2010; Wagstaff et al., 2016; Fernandez-Antoran et al., 2019). Accordingly, we have
470 suggested that in mammals, p53 takes on cell competition aspects of the Xrp1 function
471 in *Drosophila* (Baker et al., 2019). Consistent with this, p53 mediates the removal of
472 aneuploid cells in mammals, which Xrp1 does in *Drosophila* (Singla et al., 2020; Ji et al.,
473 2021a). If p53 eliminates aneuploid cells in mammals by Rp gene dose-dependent cell
474 competition, as Xrp1 does in *Drosophila*, then dual roles for mammalian p53 could both
475 contribute to tumor suppression, as dual roles for Xrp1 maintain genome integrity in

476 *Drosophila*. Consistent with this, analyses of early cancer development in a mouse
477 pancreatic cancer model indicate that losses of single chromosomes or parts of
478 chromosomes are very early steps in the progression toward transformation (Baslan et
479 al., 2022). Mammalian cells with such small-scale monosomies only seem to survive in
480 the absence of p53 (Chunduri et al., 2021). Although further studies will be required to
481 confirm the suggestion, the observations are all consistent with the possibility that by
482 contributing to genome integrity at the tissue level after the initial repair of DNA damage,
483 cell competition could represent a significant tumor-suppressive process in mammals
484 (Baker & Montagna, 2022).
485
486
487 ACKNOWLEDGEMENTS
488 We thank Drs. J. Secombe, M. Kiparaki, S. Nair, A. Kumar, and S. Muliyil for
489 comments on an earlier version of the manuscript. Fly stocks were obtained from the
490 Bloomington Drosophila Stock Center (supported by NIH P40OD018537) and the Vienna
491 Drosophila Resource Center. Confocal microscopy was performed in the Analytical
492 Imaging Facility of the Albert Einstein College of Medicine (supported by the NCI
493 P30CA013330) using the Leica SP8 microscope acquired through NIH SIG 1S10
494 OD023591. The monoclonal antibody mAb40-1a developed by J. R. Sanes was obtained
495 from the Developmental Studies Hybridoma Bank, created by the NICHD and maintained
496 at the University of Iowa, Department of Biology, Iowa City, IA 52242. This project was
497 supported by a grant from the National Institutes of Health (R01-CA284362 to NEB). Part
498 of this work is supported by the Division of Intramural Research at the National Heart,
499 Lung, and Blood Institute within the National Institutes of Health (1ZIAHL006126 to NMR).
500
501 **Disclaimer**
502 Part of this research was supported by the Intramural Research Program of the National
503 Institutes of Health (NIH). The contributions of the NIH authors were made as part of their
504 official duties as NIH federal employees, are in compliance with agency policy
505 requirements, and are considered Works of the United States Government. However, the
506 findings and conclusions presented in this paper are those of the authors and do not

507 necessarily reflect the views of the NIH or the U.S. Department of Health and Human
508 Services.
509
510 MATERIAL AND METHODS
511 **1. Fly husbandry:** Flies were raised at 25°C on standard cornmeal and molasses
512 medium, containing the following ingredients per 1L: 18g yeast; 22g molasses; 80g malt
513 extract; 9g agar; 65g cornmeal; 2.3g methyl para-benzoic acid; 6.35ml propionic acid.
514 Larvae were not distinguished for their sex before dissection.
515
516 **2. DNA damage γ-radiation treatment:** Flies were grown in the standard cornmeal
517 medium at 25°C. After egg laying was done for 24 hours, the flies were transferred to a
518 fresh vial. Following this, the larvae were allowed to grow until the wandering late III instar
519 stage, and DNA damage was induced by treating them with γ-radiation from cesium-137
520 using a Shepherd irradiator. For most experiments, 1500 Rads were administered, and
521 dissection was performed at a specified time point after the irradiation.
522
523 **3. Cell death quantification:** Cell death was quantified by counting the number of Dcp-
524 1 positive cells with the help of the ImageJ cell counter plugin. For UAS-Gal4 experiments,
525 Dcp-1 positive cells in Gal4 to the control compartment were counted and compared as
526 the ratio across different genetic perturbations. In the case of mutant wing discs, the
527 number of Dcp-1 positive cells was counted in the entire disc, and the absolute number
528 was compared.
529
530 **4. Immunohistochemistry:** Imaginal discs were fixed using 4% formaldehyde in 1× PBS,
531 followed by 2 h blocking with 0.5% bovine serum albumin (BSA) dissolved in 0.1% PBST
532 (1×PBS with 0.1% Triton X-100). Primary antibody incubations were performed at 4°C
533 overnight, followed by 2 hours of secondary incubation at room temperature. All washes
534 following antibody incubation were performed in 0.1% PBST. Primary antibodies were
535 against rabbit anti-cleaved Dcp-1 (Cell Signaling 9578, 1:200), mouse anti-γH2Av (DSHB
536 UNC93-5.2.1, 1:50), mouse anti-βGalactosidase (DSHB 40a-1, 1:50), mouse anti-p53
537 (DSHB 25F4, 1:50), and mouse anti-GFP (DSHB 12A6, 1:50), mouse anti-HA (CST 2367,

538 1:100), and anti-Xrp1 (1:250; gift from Rio lab). Alexa-Fluor (Thermo Fisher-Invitrogen)
539 and Cyanine dye (Jackson labs) conjugated secondary antibodies were used at 1:200
540 dilution. Image acquisition was performed on the Leica-Sp8 microscope, intensity
541 adjustments were made using Photoshop CC 2018, and Image J was used for image
542 processing.

543 Previous experiments have supported that significant results could be obtained
544 from 5 replicates; in most cases, more than 5 samples were analyzed. Experiments were
545 repeated at least 2 times or more for most of the results. No exclusion of the data points
546 was made while performing statistical significance. For the quantitative data, N values are
547 indicated in the figure legends. Statistical significance was performed using a Student's
548 t-test for independent or dependent means, as shown in the figure legends. For specific
549 data sets, one-way ANOVA with Post Hoc Turkey HSD was performed, as mentioned in
550 the figure legends. Exact p-values are indicated in the figures.

551

552 **5. q-RT PCR:**

553 Total RNA was extracted from wing imaginal discs of late-third instar larvae treated
554 with 2000 Rads of IR; untreated larvae were taken as a control for normalization. Wing
555 discs were collected in TRIzol reagents (Ambion), and RNA was isolated according to the
556 manufacturer's instructions. RNA samples were DNase-treated according to the
557 manufacturer's instructions (Thermo Fisher; AM1907) and reverse transcribed using the
558 Verso cDNA Synthesis Kit (Thermo Fisher; AB1453). The cDNA was used to perform the
559 q-RT PCR reactions following the manufacturer's instructions for the TaqMan^{TM} Fast
560 Advanced Master Mix (Thermo Fisher; 4444557). Custom design FAM-MGB TaqMan
561 probes were utilized for q-RT-PCR. The gene expression values were normalized to the
562 housekeeping gene RpL32 and confirmed with actin as a second control (data not
563 included). The following calculations were used for estimating fold change in gene
564 expression Δ: Ct = Ct (gene of interest) – Ct (housekeeping gene), $\Delta\Delta$Ct = ΔCt (3-4 hr IR)
565 – ΔCt (untreated average), and Fold gene expression = 2^ -($\Delta\Delta$Ct). 3 biological replicates
566 were analysed for each condition and genotype. The gene expression analysis was
567 performed using technical triplicates for each sample. It has been previously established
568 that significant results can obtained 3 biological and 3 technical triplicates.

The following TaqMan probes were used in this study:

1. p53 Dm02154335_g1
2. Xrp1 Dm02142088_g1
3. rpr Dm01823054_s1
4. hid Dm01823031_m1
5. GstD1 Dm02362792_s1
6. eiger Dm01794373_m1
7. rad50 Dm01817359_g1
8. PolZ1 Dm01843262_g1
9. DNAlig4 Dm01838632_g1
10. Ku80 Dm01791676_g1
11. *Drosophila* RpL32 Dm02151827_g1
12. *Drosophila* actin Dm02361909_s1

609 FIGURES AND FIGURE LEGENDS:

610

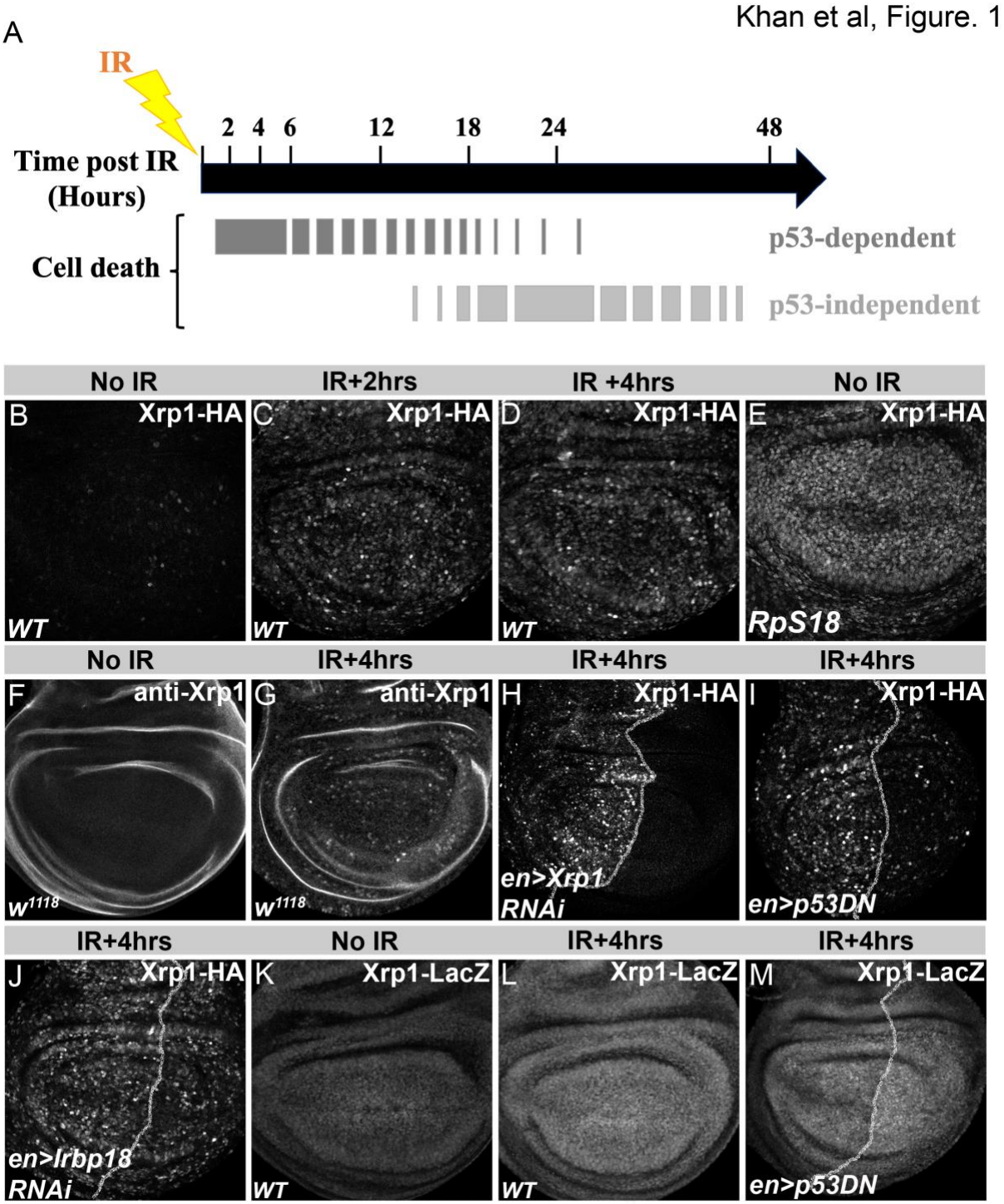

611

612 **Figure 1: DNA damage induced Xrp1 expression**

613 (A). Schematic of the approximate timeline of p53-dependent and p53-independent
614 apoptotic responses following irradiation, based on previous work (Brodsky et al., 2004;
615 Wells et al., 2006; McNamee & Brodsky, 2009; Ji et al., 2021b). (B). Xrp1 protein levels
616 in the wild type III instar wing discs stained for HA, in 0 Rads (control) (C), 2 hours after
617 1500 Rads (D), 4 hours after 1500 Rads (E), and in *Rp18*$^{+/-}$ mutant (F). Larval wing discs
618 stained with Xrp1 antibody, 0 Rads (control) (G), and 4 hours after 1500 Rads (H) (note:
619 Xrp1 antibody shows higher background than Xrp1-HA). Xrp1-HA expression at 4 hours
620 post-1500 Rads in the posterior compartment, compared relative to the anterior
621 compartment, taken as an internal control, *en-Gal4* driving *UAS-Xrp1* RNAi (I), p53
622 dominant negative (*UAS-p53*^{H159N}) (J), and *UAS-Irbp18* RNAi (K). III instar wing discs
623 assayed for *Xrp1*^{02515}-lacZ enhancer trap expression detected by anti-βgal antibody in 0
624 Rads (L), 4 hours after 1500 Rads (M), and in the wing disc expressing *UAS-p53*^{H159N}
625 under control of *en-Gal4,* 4 hours after 1500 Rads (N). N=7-8 discs were analyzed for
626 every genotype, and each experiment was repeated at least 2-3 times.
627 Genotypes: (B-D) *Xrp1-HA*, (E) *p{hs:FLP}; FRT42 RpS18 p{ubi:GFP},* (F-G) *w*^{1118} (H) *en-*
628 *Gal4::UAS-RFP, UAS-Xrp1 RNAi* (VDRC 107860)*; Xrp1-HA,* (I) *en-Gal4::UAS-RFP,*
629 *UAS-p53DN*^{H159N} (Bl. 8420)*; Xrp1-HA*, (J) *en-Gal4::UAS-RFP, UAS-Irbp18 RNAi; Xrp1-*
630 *HA*, (K-L) *P{PZ}Xrp1*^{02515}, (M) *en-Gal4::UAS-RFP,UAS-p53DN*^{H159N} (Bl. 8420);
631 *P{PZ}Xrp1*^{02515}
632

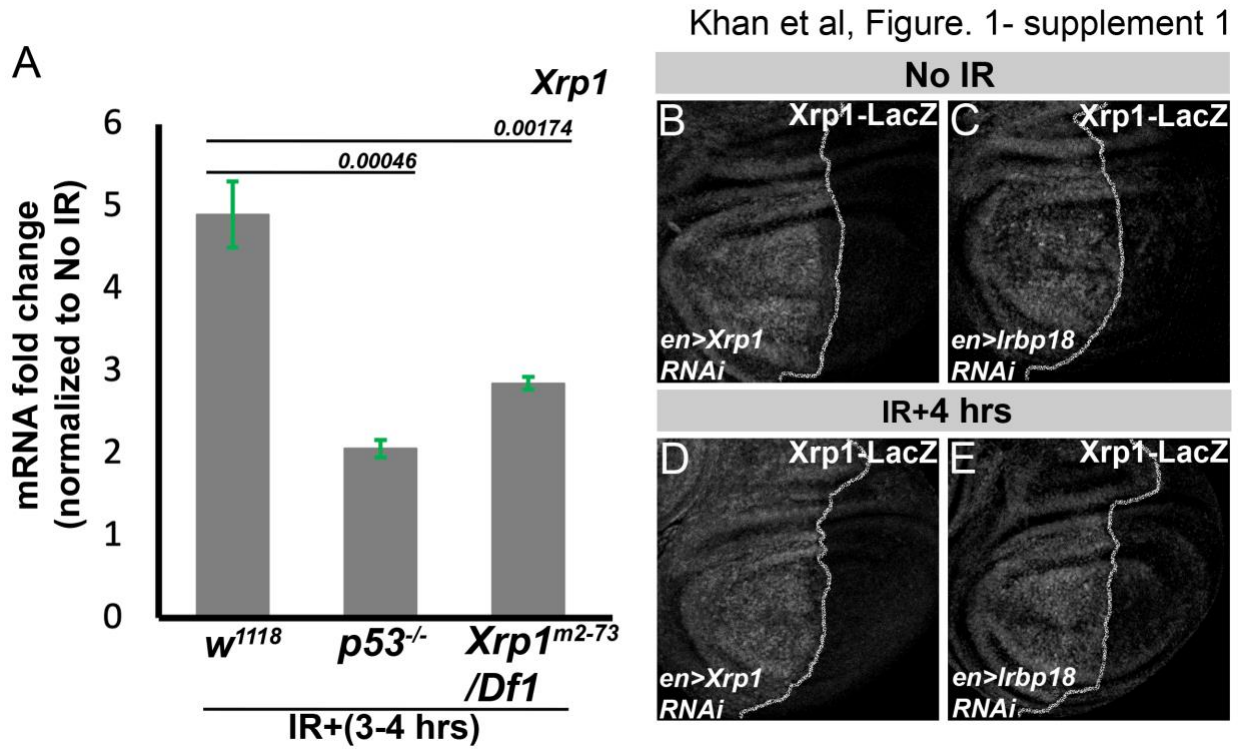

633

634 **Figure 1- Supplement 1: Xrp1 RNA expression in response to DNA damage**

635 qRT-PCR analysis for Xrp1 mRNA expression levels from III instar wing discs from the
636 genotypes w^{1118}, $p53^{[5A-1-4]}$, and $Xrp1^{m2-73}/Df1$ collected 3-4 hours after irradiation (1500
637 RADs) and normalized to an untreated (0 RADs) sample (A). III instar wing discs assayed
638 for $Xrp1^{02515}$-lacZ enhancer trap expression by anti-βgal antibody in 0 Rads for *en>Xrp1*
639 *RNAi* (B), *en>Irbp18 RNAi* (C), and 4 hours after 1500 Rads treatment in genotypes
640 *en>Xrp1 RNAi* (D), *en>Irbp18 RNAi* (E). Number of wing discs analyzed for genotypes
641 was N=3 for B, N=2 for C, N=3 for D, and N=5 for E Data is plotted as mean± SEM, and
642 a two-tailed student t-test for independent means was performed for statistical
643 significance.

644 Genotype: (A) w^{1118}, *yw;* $p53^{[5A-1-4]}$, and $Xrp1^{m2-73}$/ *Df 1*, (B & C) *en-Gal4::UAS-RFP, UAS-*
645 *Xrp1 RNAi* (VDRC 107860); *P{PZ}*$Xrp1^{02515}$ (C & E) *en-Gal4::UAS-RFP, UAS-Irbp18*
646 *RNAi*; *P{PZ}*$Xrp1^{02515}$

647

Khan et al, Figure. 2

A

B

Gene category	Radiation induced p53- dependent genes (RIPD)	Common upregulated target genes between p53- RIPD and Xrp1 dependent genes from *Rp*$^{+/-}$ mutant RNA-seq data
Transcription factors	***Xrp1, Irbp18/CG6272***, *escl*	***Xrp1, Irbp18/CG6272***
Pro-apoptotic genes	***rpr, hid***, *skl, Corp, eiger, RnrL*	***rpr, hid***
DNA repair genes	***Irbp, Ku80, rad50, mre11, mus201, mus205, lig3, lig4, RpA-70, agt,, CG6171, CG5664***, *CG13204*	***Irbp, Ku80, rad50, mre11, mus201, mus205, lig3, lig4, RpA-70, agt, CG6171, CG5664***
Redox genes	***CG9836/ISCU, CG11897***, *GstD5, spo, CG1718, pyd*	***CG9836/ISCU, CG11897***
Others	***Cul-2***, *Pka-C3*, ***eIF6, CG18596***, *halo, cyp301a1, CG12194, CG15479, CG15658, CG10965, CG16815, CG5202, CG15480, CG13714*	***Cul-2, eIF6, CG18596***

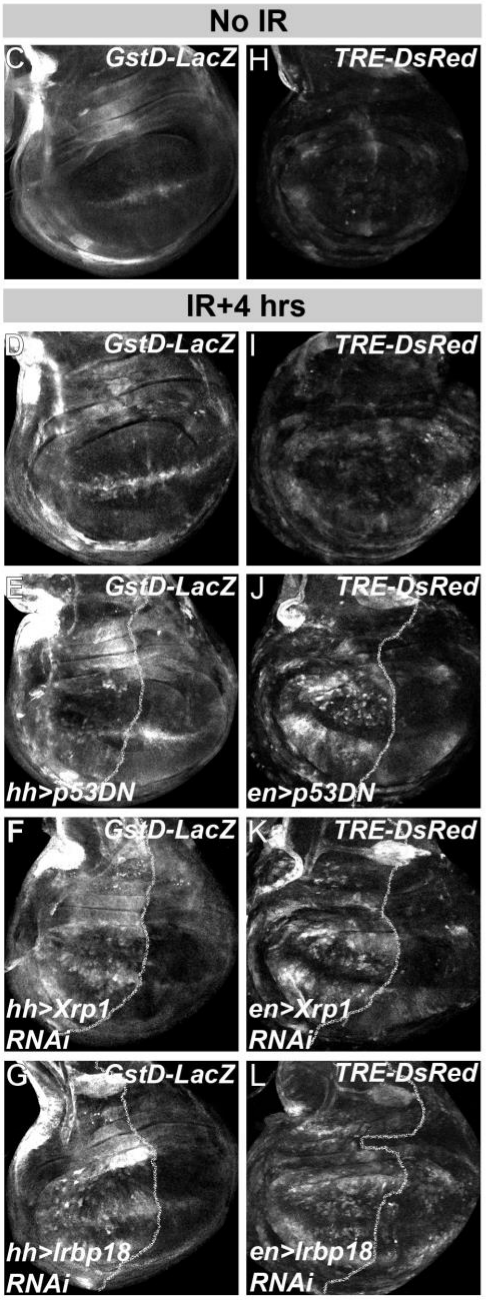

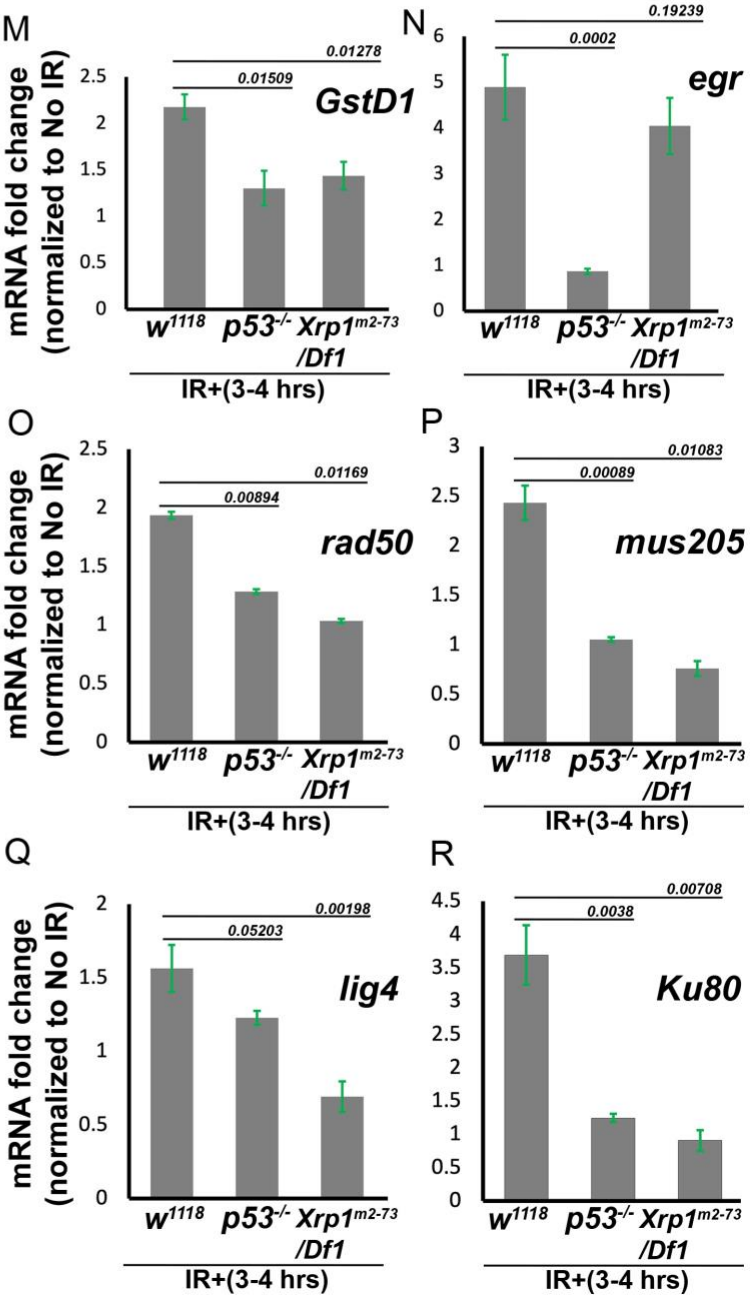

648

649 **Figure 2: Xrp1 serves as the effector of p53 in DNA damage response**
650 Vein diagram showing the overlap of p53 (Brodsky et al., 2004; Akdemir et al., 2007) and
651 Xrp1 (Baillon et al., 2018; Lee et al., 2018b) target genes (A). The table shows the genes
652 organized according to GO categories from radiation-induced p53-dependent (RIPD) and
653 genes common between Xrp1- and p53-dependent transcription programs (highlighted in
654 bold) (B). Expression of *GstD*-lacZ in III instar wing discs measured by staining for anti-
655 βgal antibody, in the wild type (no IR) (C), 4 hours after 2000 Rads in wild type disc (D),
656 *UAS-p53^{H159N}* (E), *UAS-Xrp1 RNAi* (F), and *UAS-Irbp18* RNAi (G). Expression of *TRE-*
657 *dsRed* in III instar wing discs measured by staining for anti-RFP antibody, in the wild type
658 (no IR) (H), 4 hours after 1500 Rads in wild type disc (I), *UAS-p53^{H159N}* (J). *UAS-Xrp1*
659 *RNAi* (K) and *UAS-Irbp18 RNAi* (L). qRT-PCR analysis for mRNA expression levels from
660 III instar wing discs of *w^{1118}*, *p53$^{[5A-1-4]}$* and *Xrp1^{m2-73}/Df1* collected 3-4 hours after
661 irradiation (1500 RADs) and normalized to untreated (0 Rads) sample, for the following
662 genes *GstD1* (M), *egr* (N), *rad50* (O), *mus205* (P), *lig4* (Q) and *Ku80* (R). N=7-8 discs
663 were analyzed for every genotype, and each experiment was repeated at least 2-3 times.
664 Data is plotted as mean± SEM, a two-tailed student t-test for independent means, was
665 performed for statistical significance.
666 Genotype: (C & D) *GstD-LacZ,* (E) *GstD-LacZ, UAS-p53^{H159N}* (Bl. 8420)*; hh-Gal4::UAS-*
667 *GFP,* (F) *GstD-LacZ, UAS-Xrp1 RNAi* (VDRC 107860)*; hh-Gal4::UAS-GFP,* (G) *GstD-*
668 *LacZ, UAS-Irbp18 RNAi; hh-Gal4::UAS-GFP*, (H and I) *TRE-dsRed,* (J) *TRE-dsRed::en-*
669 *Gal4, UAS-p53^{H159N}* (Bl. 8420), (K) *TRE-dsRed::en-Gal4, UAS-Xrp1 RNAi* (VDRC
670 107860), (L) *TRE-dsRed::en-Gal4, UAS-Irbp18 RNAi*, (M-R) *w^{1118}*, *yw; p53$^{[5A-1-4]}$,* and
671 *Xrp1^{m2-73}/Df1*
672

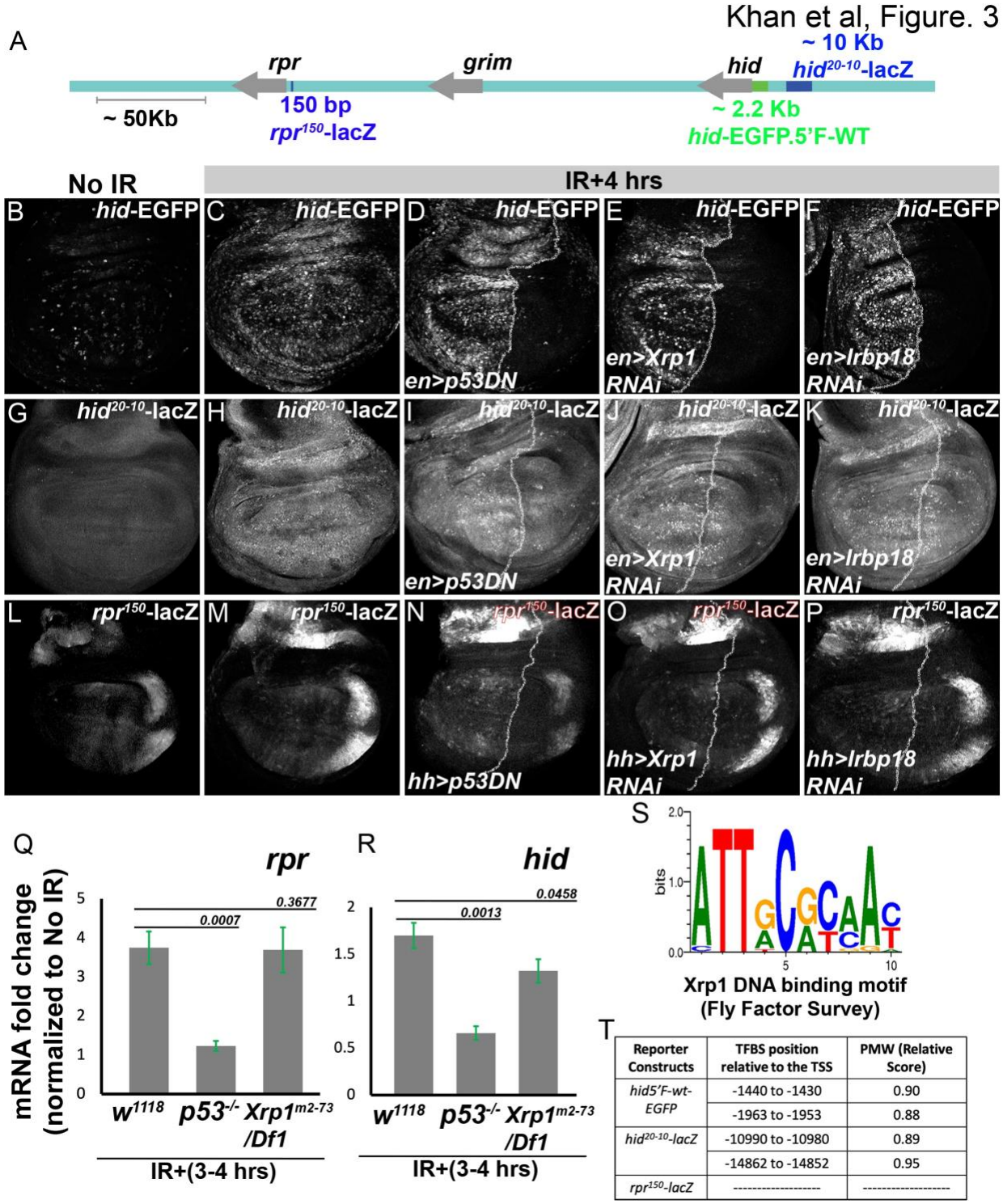

Reporter Constructs	TFBS position relative to the TSS	PMW (Relative Score)
hid5'F-wt-EGFP	-1440 to -1430	0.90
	-1963 to -1953	0.88
hid20-10-lacZ	-10990 to -10980	0.89
	-14862 to -14852	0.95
rpr150-lacZ	----------	----------

Figure 3: Xrp1 controls the expression of the regulatory sequences of the pro-apoptotic gene *hid*

Schematic of H99 locus with approximate positions of the *rpr, hid,* and *grm* and the reporter lines used for the analysis (A). Expression of *hid5'F-wt-EGFP* measured by

678 staining for anti-GFP antibody, in the wild type (no IR) (B) and 4 hours after 2000 Rads in
679 the wild type wing disc (C), *UAS-p53*^{H159N} (D), *UAS-Xrp1 RNAi* (E), and *UAS-Irbp18* RNAi
680 (F). *hid*$^{20-10}$*-lacZ* expression measured by anti-βgal staining in the wild type (no IR) (G)
681 and 4 hours after 2000 Rads in wild type wing disc (H), *UAS-p53*^{H159N} (I), *UAS-Xrp1* (J),
682 and *UAS-Irbp18* RNAi (K). *rpr*^{150}*-lacZ* expression measured by anti-βgal staining, in the
683 wild type (no IR) (L) and 4 hours after 2000 Rads in the wild type wing disc (M). *UAS-*
684 *p53*^{H159N} (N), *UAS-Xrp1* (O), and *UAS-Irbp18* RNAi (P). qRT-PCR analysis for mRNA
685 expression levels from III instar wing discs of *w*^{1118}, *p53*$^{[5A-1-4]}$, and *Xrp1*$^{m2-73}$*/Df1* collected
686 3-4 hours after irradiation (1500 RADs) and normalized to untreated (0 Rads) sample, for
687 the following genes, *rpr* (Q), and *hid* (R). Putative DNA binding motif of Xrp1/Irbp18
688 heterodimer, adapted from Fly Factor Survey (S). Position of Xrp1/Irbp18 DNA motif in
689 the upstream regulatory region of *hid* relative to the TSS (T). N=5-8 discs were analyzed
690 for every genotype; data was plotted as mean± SEM, and a two-tailed student t-test for
691 independent means was performed for statistical significance.
692 Genotype: (B & C) *hid5'F-wt-EGFP*, (D) *hid5'F-wt-EGFP; en-Gal4::UAS-RFP, UAS-*
693 *p53*^{H159N} (Bl. 8420), (E) *hid5'F-wt-EGFP; en-Gal4::UAS-RFP, UAS-Xrp1 RNAi* (VDRC
694 107860), (F) *hid5'F-wt-EGFP; en-Gal4::UAS-RFP, UAS-Irbp18 RNAi*, (G & H) *yw*; *hid*$^{20-}$
695 ^{10}*-lacZ*, (I) *en-Gal4::UAS-RFP, UAS-p53*^{H159N} (Bl. 8420)*; hid*$^{20-10}$*-lacZ*, (J) *en-Gal4::UAS-*
696 *RFP, UAS-Xrp1 RNAi* (VDRC 107860)*; hid*$^{20-10}$*-lacZ*, (K) *en-Gal4::UAS-RFP, UAS-Irbp18*
697 *RNAi; hid*$^{20-10}$*-lacZ*, (L & M) *rpr*^{150}-lacZ, (N) *rpr*^{150}*-lacZ, UAS-p53*^{H159N} (Bl. 8420)*; hh-*
698 *Gal4::UAS-GFP*, (O) *rpr*^{150}*-lacZ, UAS-Xrp1 RNAi* (VDRC 107860)*; hh-Gal4::UAS-GFP,*
699 (P) *rpr*^{150}*-lacZ, UAS-Irbp18 RNAi; hh-Gal4::UAS-GFP*, (Q-R) *w*^{1118}, *yw; p53*$^{[5A-1-4]}$, and
700 *Xrp1*$^{m2-73}$*/Df1*
701

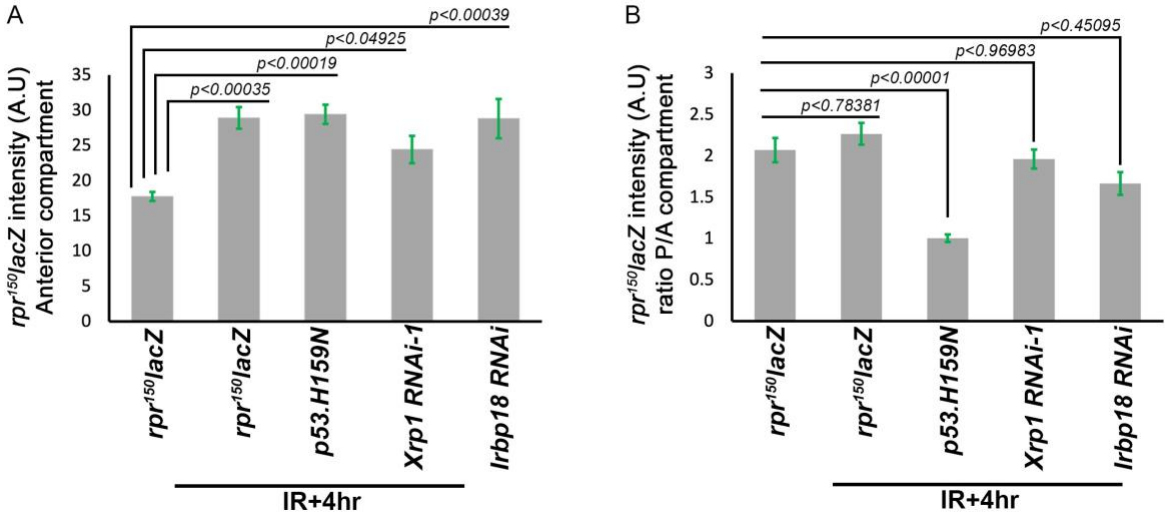

Figure 3- Supplement: *rpr^{150}lacZ* intensity quantification

(A) Average intensity quantification for *rpr^{150}lacZ* from the wing, the anterior compartment of the wing pouch, with and without IR for the genotypes shown in Figure 3 L-P. *rpr^{150}lacZ* average intensity in the anterior compartments is elevated by IR, regardless of gene expression or depletion in the P compartments. (B) The mean posterior (P) to mean anterior (A) LacZ expression ratio for each was only reduced by p53-DN, which decreased the relative *rpr-LacZ* expression level. Statistics: Data is plotted as mean± SEM; n=5 for *irbp18* RNAi, n=7 for other genotypes; significance assessed by one-way ANOVA with Post Hoc Turkey HSD. For panel B, genotypes were compared only to the unirradiated control.

Genotype: (A & B) *rpr^{150}*-lacZ**,** *rpr^{150}-lacZ, UAS-p53^{H159N}* (Bl. 8420)*; hh-Gal4::UAS-GFP***,** *rpr^{150}-lacZ, UAS-Xrp1 RNAi* (VDRC 107860)*; hh-Gal4::UAS-GFP, rpr^{150}-lacZ, UAS-Irbp18 RNAi; hh-Gal4::UAS-GFP*

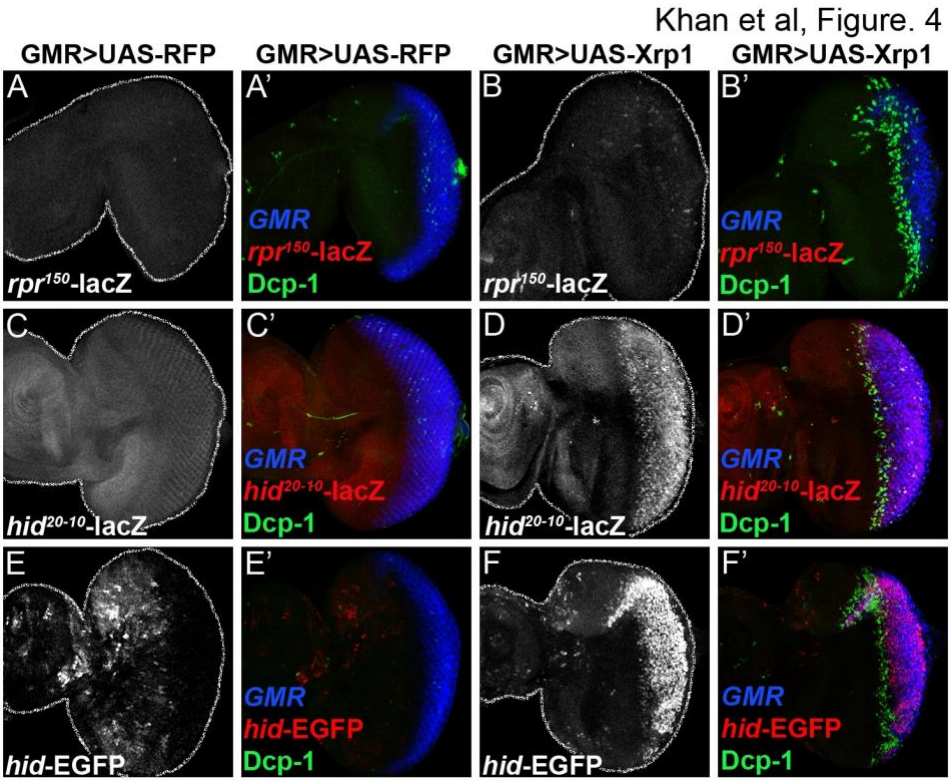

Figure 4: Xrp1 is sufficient for the expression of p53- dependent DDR target genes

rpr^{150}-lacZ reporter expression measured by anti-βgal (red) and cell death by anti-Dcp-1 (green) in III instar eye imaginal disc expressing UAS-RFP (A) and UAS-Xrp1 long isoform (B), under the control of *GMR-Gal4* (blue). *hid$^{20-10}$-lacZ* reporter expression measured by anti-βgal (red) and cell death by anti-Dcp-1 (green) in III instar eye imaginal disc expressing UAS-RFP (C) and UAS-Xrp1 long isoform (D) under the control of *GMR-Gal4* (blue). *hid5'F-wt-EGFP* reporter expression measured by anti-GFP (red) and cell death by anti-Dcp-1 (green) in III instar eye imaginal disc expressing UAS-RFP (E) and UAS-Xrp1 long isoform (F) under the control of *GMR-Gal4* (blue). N=7-8 discs were analyzed for every genotype; each experiment was repeated at least 2 times. All the control and experimental genotypes shown in this figure were kept at 18°C to lessen the effect of Xrp1 overexpression.

Genotype: (A-A') *GMR-Gal4::UAS-RFP, rpr^{150}-lacZ,* (B-B') *GMR-Gal4::UAS-RFP::UAS-Xrp1, rpr^{150}-lacZ,* (C-C') *GMR-Gal4::UAS-RFP; hid$^{20-10}$-lacZ,* (D-D') *GMR-Gal4::UAS-*

733 *RFP::UAS-Xrp1; hid$^{20-10}$-lacZ,* (E-E') *hid5'F-wt-EGFP; GMR-Gal4::UAS-RFP*, (F-F')
734 *hid5'F-wt-EGFP; GMR-Gal4::UAS-RFP, UAS-Xrp1*
735

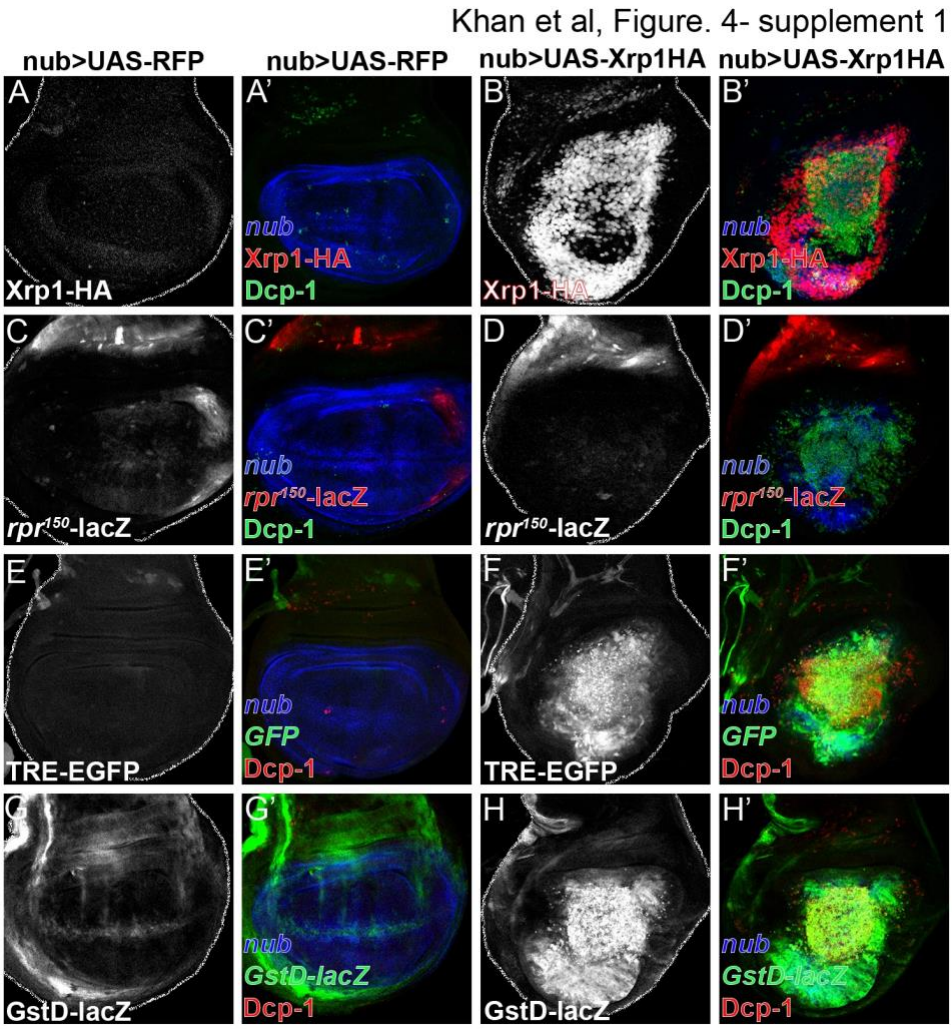

736

737 **Figure 4- Supplement 1: Xrp1 is sufficient for the expression of p53- dependent**
738 **DDR target genes**

739 Xrp1-HA protein measured by anti-HA (red) and cell death by Dcp-1 (green) in the III
740 instar wing disc expressing UAS-RFP control (A) and UAS-Xrp1 long isoform (B) under
741 the control of *nub-Gal4* (blue). *rpr^{150}-lacZ* reporter expression measured by anti-βgal
742 (green) and cell death by anti-Dcp-1 (red) in III instar wing imaginal disc expressing UAS-
743 RFP (C) and UAS-Xrp1 (D) under the control of *nub-Gal4*. *TRE-EGFP* reporter
744 expression measured by anti-GFP (green) and cell death by anti-Dcp-1 (red) in III instar
745 wing imaginal disc expressing UAS-RFP control (E) and UAS-Xrp1 (F) under the control

of *nub-Gal4* (blue). *GstD-lacZ* reporter expression measured by anti-GFP (green) and cell death by anti-Dcp-1 (red) in III instar wing imaginal disc expressing UAS-RFP (G) and UAS-Xrp1 (H) under the control of *nub-Gal4* (blue). N=7-8 discs were analyzed for every genotype, and each experiment was repeated at least 2 times. All the control and experimental genotypes shown in this figure were kept at 18°C to lessen the effect of Xrp1 overexpression.

Genotype: (A) *nub-Gal4::UAS-RFP,* (B) *nub-Gal4::UAS-RFP::UAS-Xrp1-HA,* (C) *nub-Gal4::UAS-RFP, rpr*^{150}*-lacZ,* (D) *nub-Gal4::UAS-RFP::UAS-Xrp1-HA, rpr*^{150}*-lacZ,* (E) *nub-Gal4::UAS-RFP, TRE-GFP,* (F) *nub-Gal4::UAS-RFP::UAS-Xrp1-HA, TRE-GFP,* (G) *nub-Gal4::UAS-RFP, GstD-lacZ,* (H) *nub-Gal4::UAS-RFP::UAS-Xrp1-HA, GstD-lacZ*

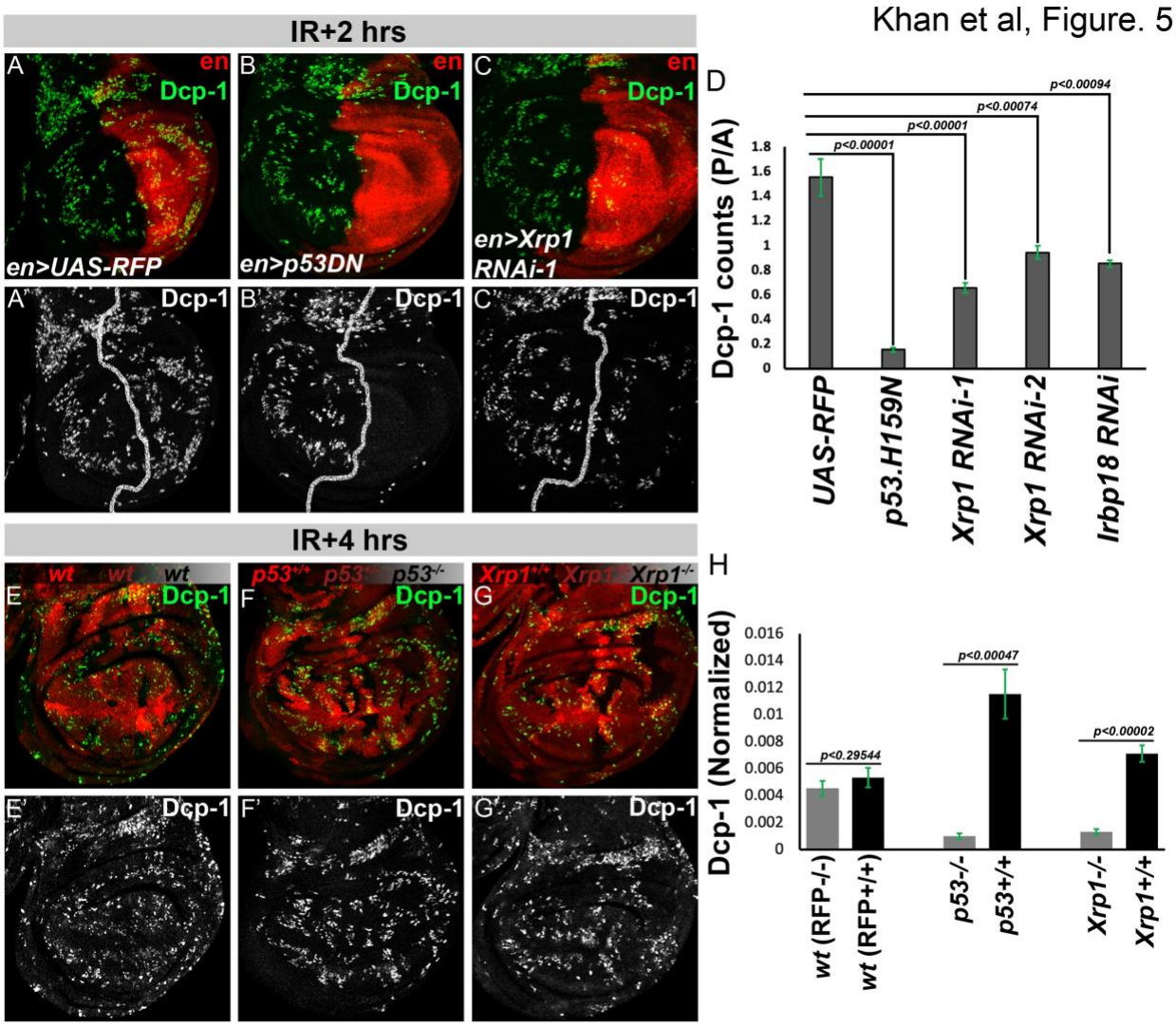

758 **Figure 5: Xrp1 is partly required for DNA damage-induced cell death**
759 *Drosophila* III instar wing imaginal discs dissected at 2 hours after 1500 Rads, cell death
760 is measured by Dcp-1 (green and grayscale) in different genetic perturbations using en-
761 Gal4 (posterior compartment (red)), UAS-RFP (A), *UAS-p53*^{H159N} (B), and *UAS-Xrp1*
762 RNAi (C). Dcp-1 positive cells were quantified and plotted as the ratio of Dcp-1 positive
763 cells in posterior (P) to anterior (A) compartments (D). Wing discs were dissected 4 hours
764 after 1500 RADs and stained for Dcp-1 positive cells in *FRT82* (E), *FRT82p53*$^{[5A-1-4]}$ (F),
765 and *FRT82Xrp1*$^{m2-73}$ (G). (H) Dcp-1 positive cells were quantified in the clone (RFP-/-)
766 and in the sister clone (RFP+/+). A 4-hour timepoint was taken to have a uniform
767 distribution of Dcp-1 positive cells. Statistics: (A-D) N=15 for each genotype. (E-H) N=8
768 for each genotype. Data is plotted as mean± SEM, a two-tailed student t-test for
769 independent means for (A-D) and dependent means for (E-H), was performed for
770 statistical significance.
771 Genotype: (A) *en-Gal4::UAS-RFP,* (B) *en-Gal4::UAS-RFP, UAS-p53DN*^{H159N} (Bl. 8420),
772 (C) *en-Gal4::UAS-RFP, UAS-Xrp1 RNAi* (Bl. 4521), (E) *p{hs:FLP}; FRT82-RFP/FRT82*
773 (30 min hs, 48 hr A.E.L), (F) *p{hs:FLP}; FRT82-RFP/FRT82-p53*$^{[5A-1-4]}$ (30 min hs, 48 hr
774 A.E.L), (G) *p{hs:FLP}; FRT82-RFP/FRT82-Xrp1*$^{m2-73}$ (30 min hs, 48 hr A.E.L)
775

Khan et al, Figure. 5- supplement 1

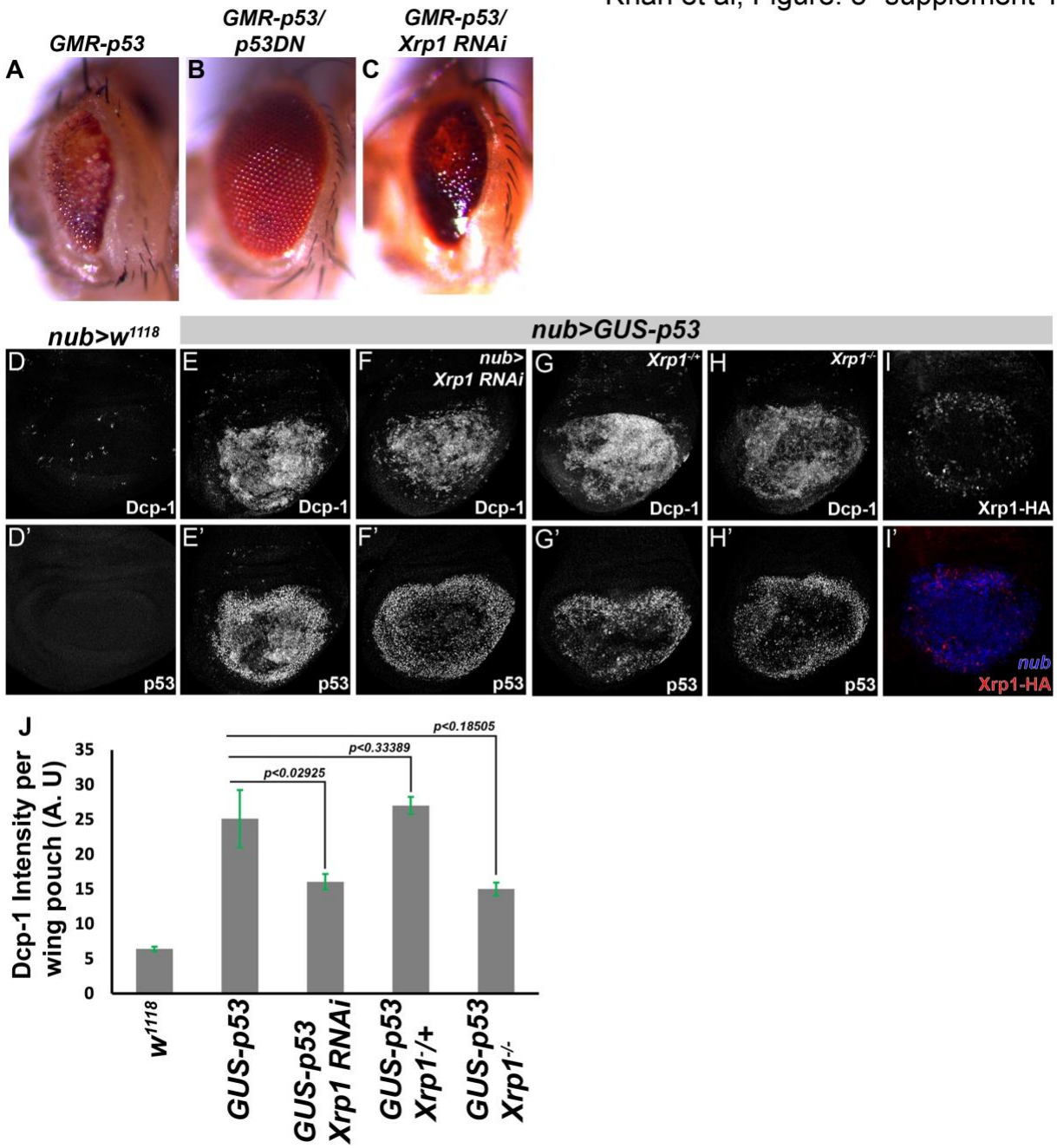

Figure 5- Supplement: Xrp1 do not rescue p53 O/E phenotype

(A) Bright field photograph of *Drosophila* eye, rough eye phenotype due to constitutive expression of p53 under the control of GMR-promoter (*GMR-p53*). (B) Overexpression of dominant-negative p53 (*UAS-p53^{H159N}*) rescues the rough eye phenotype. (C) Xrp1 knockdown by RNAi has a slight effect on the rough eye phenotype. (D) Control *nub-Gal4* exhibits few Dcp-1 positive cells, and no p53 protein was detected by anti-p53 antibody.

783 (E) *nub-Gal4* driving p53 overexpression (*GUS-p53*) in the wing pouch exhibits elevated
784 cell death measured by Dcp-1 and p53 protein, measured by anti-p53 antibody. (F) Co-
785 expressing *UAS-Xrp1* RNAi and *GUS-p53* under *nub-Gal4* led to a decrease in cell death
786 by approximately 50%. (G) Removing one copy by $Xrp1^{m2-73}/+$ did not affect cell death. (H)
787 Removing both copies of Xrp1 ($Xrp1^{m2-73}/Xrp1^{attp\ flox}$) results in a decrease in cell death of
788 approximately 50%. Xrp1-HA expression was assayed by an anti-HA antibody in the wing
789 disc, expressing p53 under the control of *nub-Gal4* (I & I'). (J) Dcp1 intensity was
790 quantified using ImageJ; N = 6 for each genotype. Data is plotted as mean$\pm$ SEM, two-
791 tailed student t-test for independent means. All the control and experimental genotypes
792 shown in this figure were kept at 18°C to lessen the effect of p53 overexpression.
793 Genotype: (A) *GMR-p53,* (B) *GUS-p53, GMR-Gal4; UAS-p53*^{H159N} (Bl. 4021), (C) *GUS-*
794 *p53, GMR-Gal4; UAS-Xrp1 RNAi* (Bl. 4521), (D) *nub-Gal4;* w^{1118}, (E) *nub-Gal4, GUS-*
795 *p53,* (F) *nub-Gal4, GUS-p53; UAS-Xrp1 RNAi* (Bl. 4521), (G) *nub-Gal4, GUS-p53;*
796 $Xrp1^{m2-73}/+$, (H) *nub-Gal4, GUS-p53;* $Xrp1^{m2-73}/Xrp1^{attp\ flox}$, (I) *nub-Gal4, GUS-p53; Xrp1-*
797 *HA*
798

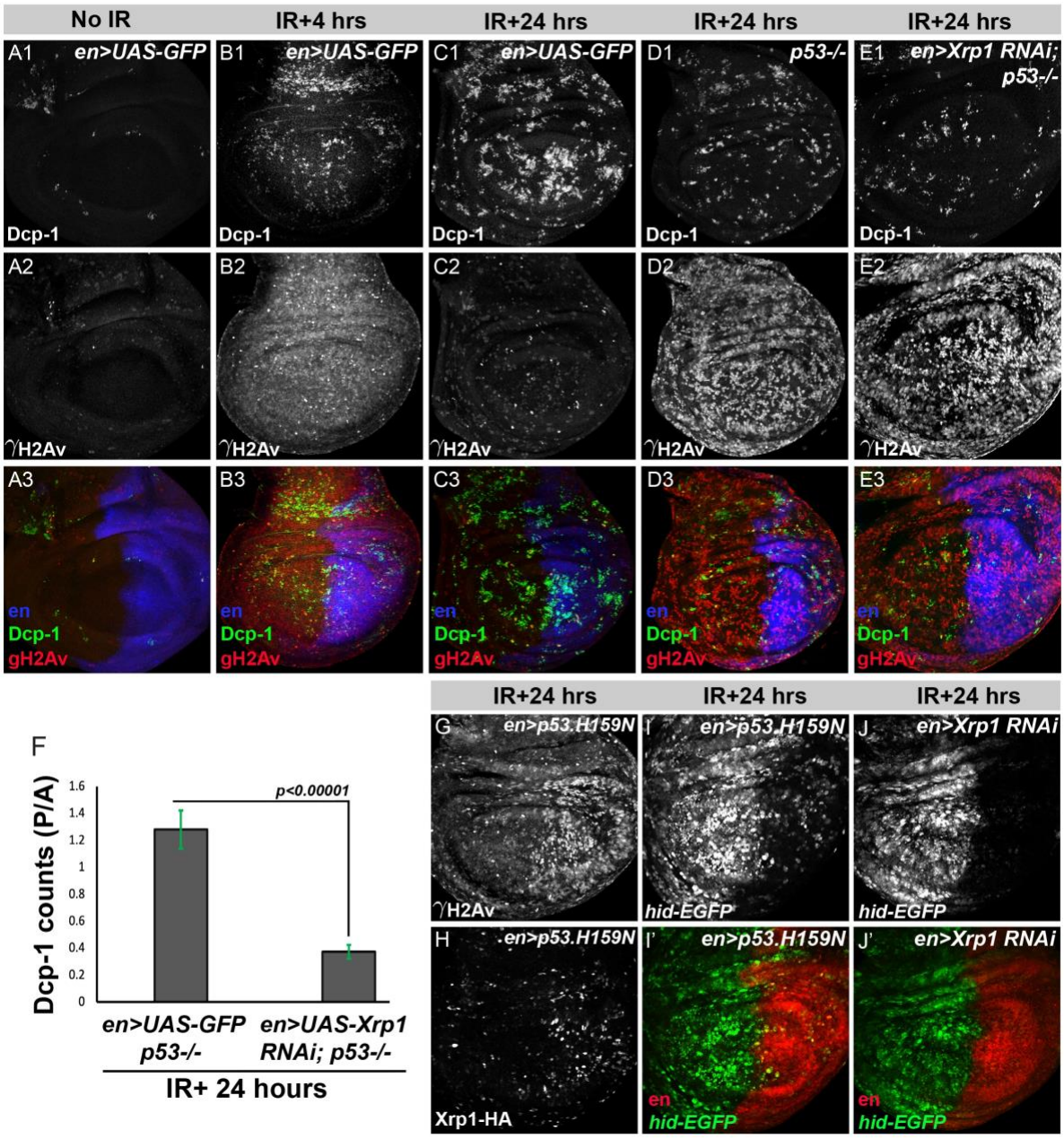

Figure 6: Xrp1 limits genomic instabilities by removing aneuploid cells in a p53-independent manner

(A-B) III instar wing disc from larvae stained for cell death (Dcp-1, green), DNA damage signaling (γH2Av, red), control (*en-Gal4, UAS-GFP*) (A), and 4 hours after 1500 Rads of γ-rays treatment (B). (C-E) III instar wing disc from larvae 24 hours after 1500 Rads of γ-rays treatment, stained for cell death (Dcp-1, green), DNA damage signaling (γH2Av, red)

806 in control (*en-Gal4, UAS-GFP*) (C), *p53*$^{-/-}$ mutant (D), and Xrp1 k/d in *p53*$^{-/-}$ mutant
807 background (E). (F) Quantification of Dcp-1 positive cells anterior versus posterior
808 compartments in *p53*$^{-/-}$ mutant and Xrp1 k/d in *p53*$^{-/-}$ mutant background. (G) γH2Av and
809 (H) Xrp1-HA levels 24 hours after irradiation in the posterior compartment of the wing disc
810 expressing *p53*^{H159N} under the control of engrailed Gal4. *hid5'F-wt-EGFP* expression in
811 *UAS-p53*^{H159N} (I) and Xrp1 RNAi K/D (J) 24 hours after irradiation. N=15 for (A-C), and
812 N=8, for (E & F). Data is plotted as mean± SEM, student t-test, two-tailed for the
813 independent sample, was performed for statistical significance.
814 Genotype: (A-B) *en-Gal4::UAS-GFP*, (C) *en-Gal4::UAS-GFP; FRT82-RFP/FRT82-p53*$^{[5A-1-4]}$,
815 (D) *en-Gal4::UAS-GFP; FRT82-RFP/FRT82-p53*$^{[5A-1-4]}$, (E) *en-Gal4::UAS-GFP, UAS-*
816 *Xrp1 RNAi* (VDRC 107860)*; FRT82-RFP/FRT82-p53*$^{[5A-1-4]}$*,* (G) *en-Gal4::UAS-RFP;*
817 *UAS-p53DN*^{H159N} (Bl. 8420)*; Xrp1-HA*, (H) *en-Gal4::UAS-RFP; UAS-p53DN*^{H159N} (Bl.
818 8420)*; Xrp1-HA*, (I) *hid5'F-wt-EGFP; en-Gal4::UAS-RFP, UAS-p53*^{H159N} (Bl. 8420)**,** and
819 (J) *hid5'F-wt-EGFP; en-Gal4::UAS-RFP, UAS-Xrp1 RNAi* (VDRC 107860)
820

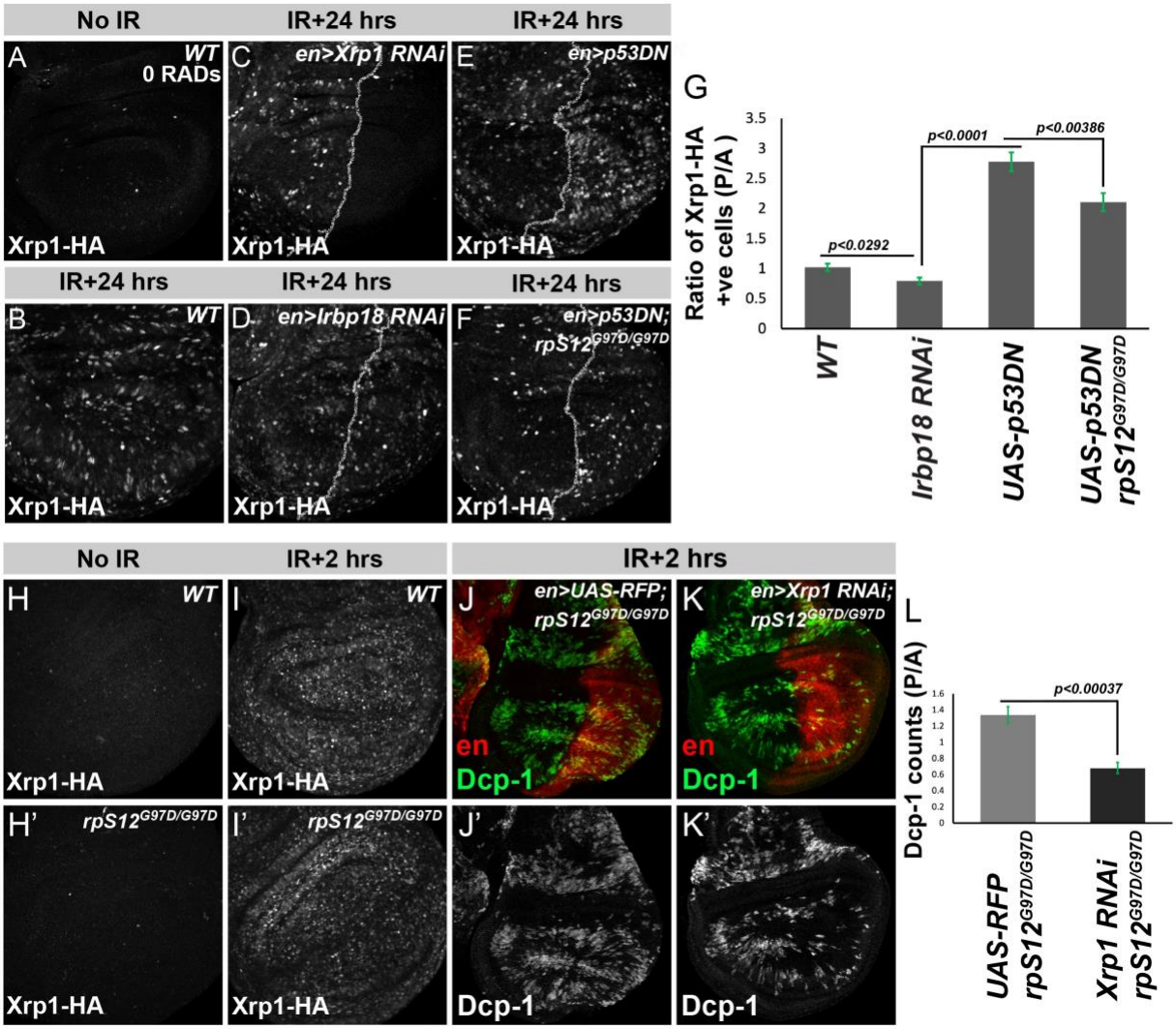

Figure 6- Supplement 1: Xrp1 induction independent of p53

(A-F) Xrp1-HA expression in control disc (A), 24 hours after 1500 rads (B), *UAS-Xrp1* RNAi (C), *UAS-Irbp1* RNAi (D), *UAS-p53*^{H159N} (E), and *UAS-p53*^{H159N} in *rpS12*$^{G97D/G97D}$ mutant background (F). (G) The ratio of Xrp1-positive cells in anterior (A) to posterior (P) compartments in *UAS-p53*^{H159N} and *UAS-p53*^{H159N} in *rpS12*$^{G97D/G97D}$ mutant background. (H-J) Cell death measured by anti-Dcp-1 (green and grayscale) in wing imaginal discs dissected at 2 hours after 1500 Rads, measured in en-Gal4 (posterior compartment (red)) versus anterior compartment *UAS-RFP; rpS12*^{G97D} (H), and *UAS-Xrp1 RNAi; rpS12*^{G97D} (I). Dcp-1 positive cells were quantified in anterior (A) and posterior (P) compartments and plotted as the P/A ratio (J). N=7 discs for (A, B, C, E, and F), N=3 discs for (D), N=6

832 discs for (J-L), data is plotted as mean± SEM, and a student t-test, two-tailed for the
833 independent sample, was performed for statistical significance.
834 Genotype: (A & B) *Xrp1-HA*, (C) *en-Gal4::UAS-RFP; UAS-Xrp1 RNAi* (VDRC 107860)*;*
835 *Xrp1-HA*, (D) *en-Gal4::UAS-RFP; UAS-Irbp18 RNAi; Xrp1-HA*, (E) *en-Gal4::UAS-RFP;*
836 *UAS-p53DN*^{H159N} (Bl. 8420)*; Xrp1-HA*, (F) *en-Gal4::UAS-RFP; UAS-p53DN*^{H159N} (Bl.
837 8420)*; Xrp1-HA-rpS12*$^{G97D/G97D}$ (H) *en-Gal4::UAS-RFP; rpS12*$^{G97D/G97D}$, (I) *en-Gal4::UAS-*
838 *RFP, UAS-Xrp1 RNAi* (VDRC 107860)*; rpS12*$^{G97D/G97D}$
839

Khan et al, Figure. 6- supplement 2

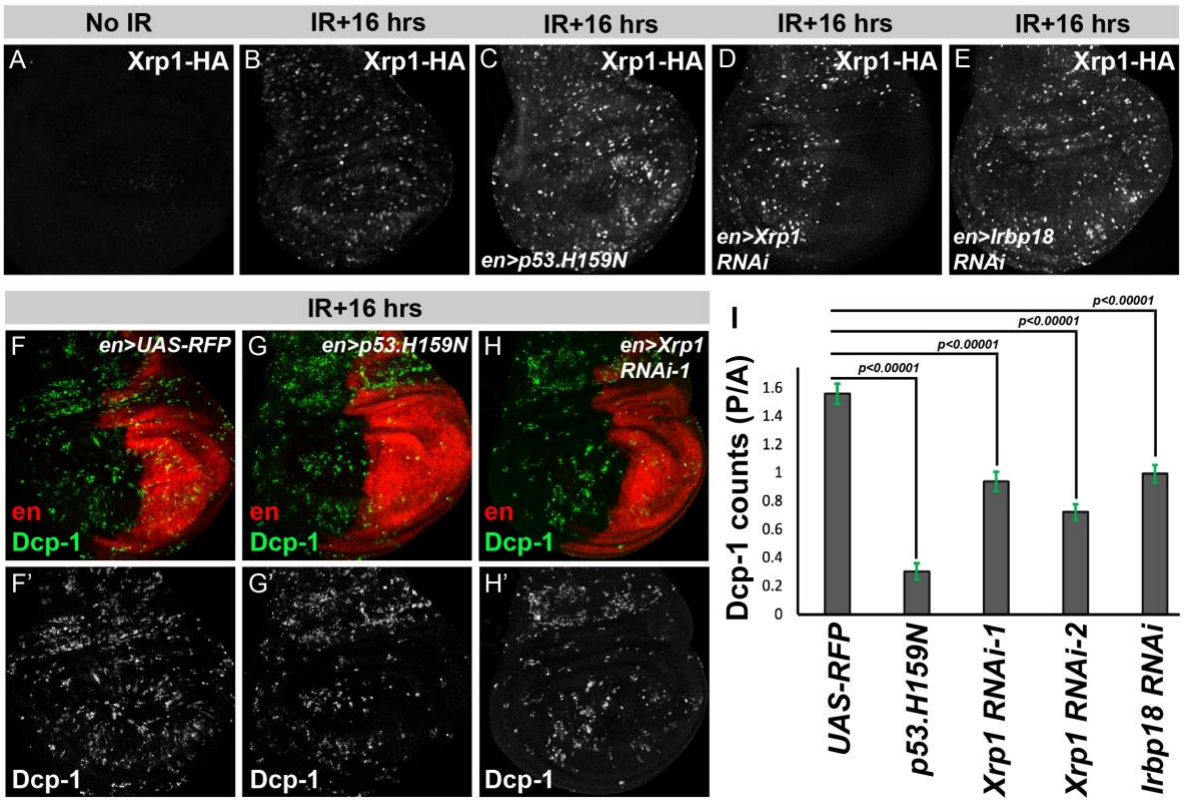

840

841 **Figure 6- Supplement 2: Induction of p53-independent DDR occurs around 16**
842 **hours post-irradiation**
843 (A-E) Xrp1-HA expression in control disc (A), 16 hours after 1500 rads (B), *UAS-p53*^{H159N}
844 (C), *UAS-Xrp1* RNAi (D), and *UAS-Irbp1* RNAi (E). *Drosophila* III instar wing imaginal
845 discs dissected at 16 hours after 1500 Rads, cell death is measured by Dcp-1 (green and
846 grayscale) in different genetic perturbations using en-Gal4 (posterior compartment (red)),
847 UAS-RFP (F), *UAS-p53*^{H159N} (G), and *UAS-Xrp1* RNAi (H). Dcp-1 positive cells were

848 quantified and plotted as the ratio of Dcp-1 positive cells in posterior (P) to anterior (A)
849 compartments (I). Dcp-1 positive cells were quantified in anterior (A) and posterior (P)
850 compartments and plotted as the P/A ratio (I). N=10 for (F-I), data is plotted as mean±
851 SEM, and a student t-test, two-tailed for the independent sample, was performed for
852 statistical significance.
853 Genotype: (A & B) *Xrp1-HA*, (C) *en-Gal4::UAS-RFP; UAS-p53DN*^{H159N} (Bl. 8420)*; Xrp1-*
854 *HA*, (D) *en-Gal4::UAS-RFP; UAS-Irbp18 RNAi; Xrp1-HA*, and (E) *en-Gal4::UAS-RFP;*
855 *UAS-Xrp1 RNAi* (VDRC 107860)*; Xrp1-HA*, (F) *en-Gal4::UAS-RFP,* (G) *en-Gal4::UAS-*
856 *RFP, UAS-p53DN*^{H159N} (Bl. 8420), (H) *en-Gal4::UAS-RFP, UAS-Xrp1 RNAi* (Bl. 4521), (I)
857 *en-Gal4::UAS-RFP, UAS-Irbp18 RNAi*
858

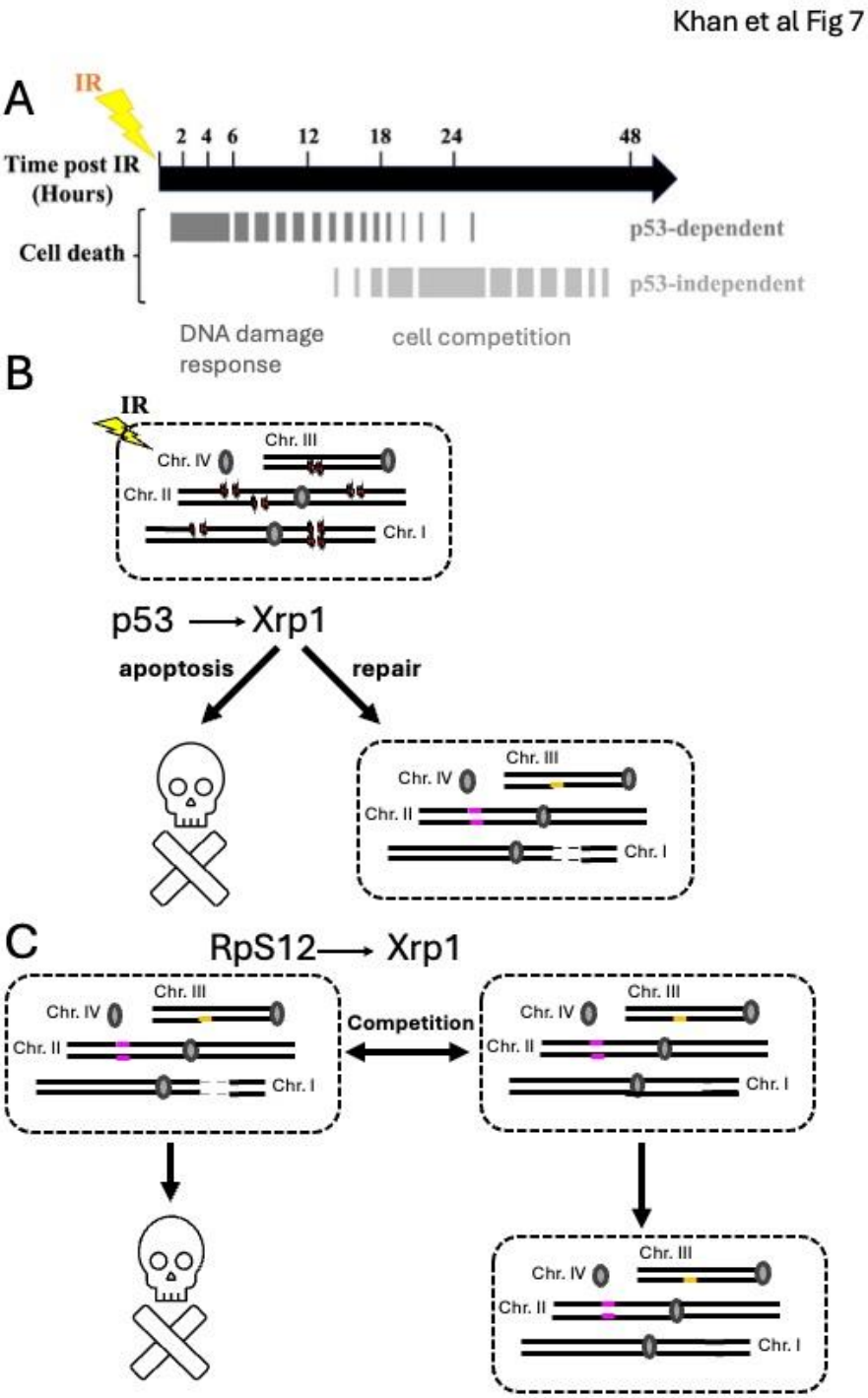

Figure 7: Model

(A) Our work reinforces the conclusion that an acute, p53-dependent apoptotic response to irradiation represents the DDR, while the later, p53-independent phase is associated

863 with elimination of aneuploid cells by cell competition. The p53-independent phase
864 depends more completely on Xrp1, whose expression at this stage is RpS12-dependent.
865 The cell competition response is enhanced when p53 is absent, resulting in prolonged
866 DNA damage and presumably an increase in aneuploidy. (B) The acute, p53-dependent
867 DDR acts in part through Xrp1 as a downstream transcription factor. The DDR results in
868 the repair of DNA damage or the removal of damaged cells by cell death. DNA repair can
869 introduce errors (colored) including chromosome aberrations resulting in loss of genetic
870 material (dashes) (C) When repair of DNA damage results in segmental aneuploidy, Xrp1
871 activation is triggered via an RpS12-dependent, p53-independent pathway that removes
872 aneuploid cells via cell competition with unaffected cells.
873

874 **Supplementary Table 1:** Key Resources Table

Key Resources Table				
Reagent type (species) or resource	**Designation**	**Source or reference**	**Identifiers**	**Additional information**
gene (*Drosophila melanogaster*)	Xrp1		FLYBASE: FBgn0261113	
gene (*Drosophila melanogaster*)	irbp18		FLYBASE: FBgn0036126	
genetic reagent (*D. melanogaster*)	p53		FLYBASE: FBgn0039044	
genetic reagent (*D. melanogaster*)	rpS12		FLYBASE: FBgn0286213	
genetic reagent (*D. melanogaster*)	*Xrp1*$^{m2\text{-}73}$	(Lee et al., 2016)	FLYBASE: FBal0346068	Bloomington Drosophila Stock Center #81270
genetic reagent (*D. melanogaster*)	*Xrp1*^{02515}	(Spradling et al., 1999)	FLYBASE: FBal0009448	Bloomington Drosophila Stock Center #11569
genetic reagent (*D. melanogaster*)	*Xrp1*$^{attP\ flox}$	(Blanco et al., 2020)		Strain maintained in Dr. Nicholas Baker's lab

genetic reagent (*D. melanogaster*)	Xrp1^{HA}	(Blanco et al., 2020)		Strain maintained in Dr. Nicholas Baker's lab
genetic reagent (*D. melanogaster*)	UAS-Xrp1 (long isoform)	(Tsurui-Nishimura et al., 2013)	FLYBASE: FBal0284387	
genetic reagent (*D. melanogaster*)	*irbp18*^{05006}	(Francis et al., 2016)	FLYBASE: FBal0185260	Exelisis Drosophila Collection #f05006
genetic reagent (*D. melanogaster*)	*rpS12*^{G97D}		FLYBASE: FBgn0286213	Strain maintained in Dr. Nicholas Baker's lab
genetic reagent (*D. melanogaster*)	*p53*$^{[5A-1-4]}$		FLYBASE: FBgn0039044	Bloomington Drosophila Stock Center #6815
genetic reagent (*D. melanogaster*)	UAS-p53.H159N.Ex-2 (Chr. II)		FLYBASE: FBti0040583	Bloomington Drosophila Stock Center #8420
genetic reagent (*D. melanogaster*)	UAS-p53.H159N.Ex -3 (Chr. III)		FLYBASE: FBti0040584	Bloomington Drosophila Stock Center #8421
genetic reagent (*D. melanogaster*)	UAS-dsRNA^{Xrp1}	(Ni et al., 2011)	FLYBASE: FBti0144696	Bloomington Drosophila Stock Center #34521

genetic reagent (*D. melanogaster*)	UAS-dsRNA^{Xrp1}		FLYBASE: FBst0479673	Vienna Drosophila Resource Center #107860
genetic reagent (*D. melanogaster*)	UAS-dsRNA^{irbp18}	(Ni et al., 2011)	FLYBASE: FBti0140125	Bloomington Drosophila Stock Center #33652
genetic reagent (*D. melanogaster*)	UAS-dsRNA^{w}	(Ni et al., 2011)	FLYBASE: FBtp0064645	Bloomington Drosophila Stock Center #33623
genetic reagent (*D. melanogaster*)	arm-LacZ	(Vincent et al., 1994)	FLYBASE: FBal0040819	
genetic reagent (*D. melanogaster*)	Ubi-GFP	(Davis et al., 1995)	FLYBASE: FBal0047085	
genetic reagent (*D. melanogaster*)	M(2)56F (mutating RpS18)	Laboratory of Y. Hiromi	FLYBASE: FBal0011916	
genetic reagent (*D. melanogaster*)	hs-FLP	(Struhl & Basler, 1993)	FLYBASE: FBtp0001101	
genetic reagent (*D. melanogaster*)	ey-FLP	(Newsome et al., 2000)	FLYBASE: FBal0098303	
genetic reagent (*D. melanogaster*)	GMR-gal4	(Freeman, 1996)	FLYBASE: FBtp0001315	
genetic reagent (*D. melanogaster*)	P{neoFRT}42D	(Xu & Rubin, 1993)	FLYBASE: FBti0141188	Bloomington Drosophila Stock Center #1802

genetic reagent (*D. melanogaster*)	P{neoFRT}80B	(Xu & Rubin, 1993)	FLYBASE: FBti0002073	Bloomington Drosophila Stock Center #1988
genetic reagent (*D. melanogaster*)	P{neoFRT}82B	(Xu & Rubin, 1993)	FLYBASE: FBti0002074	Bloomington Drosophila Stock Center #2050, 2051
Antibody	Polyclonal Rabbit anti-XRP1 (short isoform)	(Francis et al., 2016)		1:200 dilution
Antibody	Mouse anti-HA Tag monoclonal	Cell Signalling Technology	Cat #2367 RRID:AB_10691311	1:100 dilution
Antibody	Mouse anti-beta galactosidase (mAb40-1a) monoclonal	DSHB	RRID: AB_2314509	1:100 dilution
Antibody	Rabbit anti-active-Dcp1 polyclonal	Cell Signalling Technology	Cat #9578 RRID:AB_2721060	1:50 dilution
Antibody	Mouse anti-p53 (25F4) monoclonal	DSHB	RRID: AB_579787	1:20 dilution

875
876
877

878 REFERENCES

879 Akdemir, F., Christich, A., Sogame, N., Chapo, J., & Abrams, J. M. (2007). p53 directs focused
880 genomic responses in Drosophila. *Oncogene*, *26*(36), 5184-5193.
881 https://doi.org/10.1038/sj.onc.1210328

882 Allen, M. A., Andrysik, Z., Dengler, V. L., Mellert, H. S., Guarnieri, A., Freeman, J. A., Sullivan, K.
883 D., Galbraith, M. D., Luo, X., Kraus, W. L., Dowell, R. D., & Espinosa, J. M. (2014). Global
884 analysis of p53-regulated transcription identifies its direct targets and unexpected
885 regulatory mechanisms. *Elife*, *3*, e02200. https://doi.org/10.7554/eLife.02200

886 Alpar, L., Bergantinos, C., & Johnston, L. A. (2018). Spatially Restricted Regulation of Spatzle/Toll
887 Signaling during Cell Competition. *Dev Cell*, *46*(6), 706-719 e705.
888 https://doi.org/10.1016/j.devcel.2018.08.001

889 Andrysik, Z., Galbraith, M. D., Guarnieri, A. L., Zaccara, S., Sullivan, K. D., Pandey, A., MacBeth,
890 M., Inga, A., & Espinosa, J. M. (2017). Identification of a core TP53 transcriptional
891 program with highly distributed tumor suppressive activity. *Genome Res*, *27*(10), 1645-
892 1657. https://doi.org/10.1101/gr.220533.117

893 Baillon, L., Germani, F., Rockel, C., Hilchenbach, J., & Basler, K. (2018). Xrp1 is a transcription
894 factor required for cell competition-driven elimination of loser cells. *Sci Rep*, *8*(1),
895 17712. https://doi.org/10.1038/s41598-018-36277-4

896 Baker, D. J., Jin, F., Jeganathan, K. B., & van Deursen, J. M. (2009). Whole chromosome
897 instability caused by Bub1 insufficiency drives tumorigenesis through tumor suppressor
898 gene loss of heterozygosity. *Cancer Cell*, *16*(6), 475-486.
899 https://doi.org/10.1016/j.ccr.2009.10.023
900 S1535-6108(09)00387-0 [pii]

901 Baker, D. J., & van Deursen, J. M. (2010). Chromosome missegregation causes colon cancer by
902 APC loss of heterozygosity. *Cell Cycle*, *9*(9), 1711-1716.
903 https://doi.org/10.4161/cc.9.9.11314

904 Baker, N. E. (2020). Emerging mechanisms of cell competition. *Nat Rev Genet*, *21*(11), 683-697.
905 https://doi.org/10.1038/s41576-020-0262-8

906 Baker, N. E., & Kale, A. (2016). Mutations in ribosomal proteins: Apoptosis, cell competition,
907 and cancer. *Mol Cell Oncol*, *3*(1), e1029065.
908 https://doi.org/10.1080/23723556.2015.1029065

909 Baker, N. E., Kiparaki, M., & Khan, C. (2019). A potential link between p53, cell competition and
910 ribosomopathy in mammals and in Drosophila. *Dev Biol*, *446*(1), 17-19.
911 https://doi.org/10.1016/j.ydbio.2018.11.018

912 Baker, N. E., & Montagna, C. (2022). Reducing the aneuploid cell burden - cell competition and
913 the ribosome connection. *Dis Model Mech*, *15*(11).
914 https://doi.org/10.1242/dmm.049673

915 Baslan, T., Morris, J. P. t., Zhao, Z., Reyes, J., Ho, Y. J., Tsanov, K. M., Bermeo, J., Tian, S., Zhang,
916 S., Askan, G., Yavas, A., Lecomte, N., Erakky, A., Varghese, A. M., Zhang, A., Kendall, J.,
917 Ghiban, E., Chorbadjiev, L., Wu, J.,…Lowe, S. W. (2022). Ordered and deterministic
918 cancer genome evolution after p53 loss. *Nature*, *608*(7924), 795-802.
919 https://doi.org/10.1038/s41586-022-05082-5

920 Baumgartner, M. E., Dinan, M. P., Langton, P. F., Kucinski, I., & Piddini, E. (2021). Proteotoxic
921 stress is a driver of the loser status and cell competition. *Nat Cell Biol*, *23*(2), 136-146.
922 https://doi.org/10.1038/s41556-020-00627-0
923 Blanco, J., Cooper, J. C., & Baker, N. E. (2020). Roles of C/EBP class bZip proteins in the growth
924 and cell competition of Rp ('Minute') mutants in Drosophila. *Elife*, *9*.
925 https://doi.org/10.7554/eLife.50535
926 Bondar, T., & Medzhitov, R. (2010a). p53-mediated hematopoietic stem and progenitor cell
927 competition. *Cell Stem Cell*, *6*(4), 309-322. https://doi.org/10.1016/j.stem.2010.03.002
928 Bondar, T., & Medzhitov, R. (2010b). p53-mediated hematopoietic stem and progenitor cell
929 competition. *Cell Stem Cell*, *6*(4), 309-322. https://doi.org/10.1016/j.stem.2010.03.002
930 S1934-5909(10)00099-8 [pii]
931 Boulan, L., Andersen, D., Colombani, J., Boone, E., & Leopold, P. (2019). Inter-Organ Growth
932 Coordination Is Mediated by the Xrp1-Dilp8 Axis in Drosophila. *Dev Cell*, *49*(5), 811-818
933 e814. https://doi.org/10.1016/j.devcel.2019.03.016
934 Boutelle, A. M., & Attardi, L. D. (2021). p53 and Tumor Suppression: It Takes a Network. *Trends*
935 *Cell Biol*, *31*(4), 298-310. https://doi.org/10.1016/j.tcb.2020.12.011
936 Bridges, C. B., & Morgan, T. H. (1923). The third-chromosome group of mutant characters of
937 *Drosophila melanogaster*. *Carnegie Institute Publication*, *327*, 1-251.
938 Brodsky, M. H., Nordstrom, W., Tsang, G., Kwan, E., Rubin, G. M., & Abrams, J. M. (2000).
939 Drosophila p53 binds a damage response element at the reaper locus. *Cell*, *101*(1), 103-
940 113. https://doi.org/10.1016/S0092-8674(00)80627-3
941 Brodsky, M. H., Weinert, B. T., Tsang, G., Rong, Y. S., McGinnis, N. M., Golic, K. G., Rio, D. C., &
942 Rubin, G. M. (2004). Drosophila melanogaster MNK/Chk2 and p53 regulate multiple
943 DNA repair and apoptotic pathways following DNA damage. *Mol Cell Biol*, *24*(3), 1219-
944 1231. http://www.ncbi.nlm.nih.gov/pubmed/14729967
945 Brown, B., Mitra, S., Roach, F. D., Vasudevan, D., & Ryoo, H. D. (2021). The transcription factor
946 Xrp1 is required for PERK-mediated antioxidant gene induction in Drosophila. *Elife*, *10*.
947 https://doi.org/10.7554/eLife.74047
948 Bursac, S., Brdovcak, M. C., Donati, G., & Volarevic, S. (2014). Activation of the tumor
949 suppressor p53 upon impairment of ribosome biogenesis. *Biochim Biophys Acta*,
950 *1842*(6), 817-830. https://doi.org/10.1016/j.bbadis.2013.08.014
951 Chakravarti, A., Thirimanne, H. N., Brown, S., & Calvi, B. R. (2022). Drosophila p53 isoforms have
952 overlapping and distinct functions in germline genome integrity and oocyte quality
953 control. *Elife*, *11*. https://doi.org/10.7554/eLife.61389
954 Christophorou, M. A., Martin-Zanca, D., Soucek, L., Lawlor, E. R., Brown-Swigart, L., Verschuren,
955 E. W., & Evan, G. I. (2005). Temporal dissection of p53 function in vitro and in vivo. *Nat*
956 *Genet*, *37*(7), 718-726. https://doi.org/10.1038/ng1572
957 Christophorou, M. A., Ringshausen, I., Finch, A. J., Swigart, L. B., & Evan, G. I. (2006). The
958 pathological response to DNA damage does not contribute to p53-mediated tumour
959 suppression. *Nature*, *443*(7108), 214-217. https://doi.org/10.1038/nature05077
960 Chunduri, N. K., Menges, P., Zhang, X., Wieland, A., Gotsmann, V. L., Mardin, B. R., Buccitelli, C.,
961 Korbel, J. O., Willmund, F., Kschischo, M., Raeschle, M., & Storchova, Z. (2021). Systems
962 approaches identify the consequences of monosomy in somatic human cells. *Nat*
963 *Commun*, *12*(1), 5576. https://doi.org/10.1038/s41467-021-25288-x

964 Cruz, J., Sun, W. Y., Verbeke, A., & Hariharan, I. K. (2025). Single-cell transcriptomics of X-ray
965 irradiated Drosophila wing discs reveals heterogeneity related to cell-cycle status and
966 cell location. *bioRxiv*. https://doi.org/10.1101/2024.12.10.627868
967 Davis, I., Girdham, C. H., & O'Farrell, P. H. (1995). A nuclear GFP that marks nuclei in living
968 Drosophila embryos; maternal supply overcomes a delay in the appearance of zygotic
969 fluorescence. *Dev Biol*, *170*(2), 726-729. https://doi.org/10.1006/dbio.1995.1251
970 Dekanty, A., Barrio, L., & Milan, M. (2015). Contributions of DNA repair, cell cycle checkpoints
971 and cell death to suppressing the DNA damage-induced tumorigenic behavior of
972 Drosophila epithelial cells. *Oncogene*, *34*(8), 978-985.
973 https://doi.org/10.1038/onc.2014.42
974 Fan, Y., Lee, T. V., Xu, D., Chen, Z., Lamblin, A. F., Steller, H., & Bergmann, A. (2010). Dual roles
975 of Drosophila p53 in cell death and cell differentiation. *Cell Death Differ*, *17*(6), 912-921.
976 https://doi.org/10.1038/cdd.2009.182
977 cdd2009182 [pii]
978 Fernandez-Antoran, D., Piedrafita, G., Murai, K., Ong, S. H., Herms, A., Frezza, C., & Jones, P. H.
979 (2019). Outcompeting p53-Mutant Cells in the Normal Esophagus by Redox
980 Manipulation. *Cell Stem Cell*, *25*(3), 329-341 e326.
981 https://doi.org/10.1016/j.stem.2019.06.011
982 Fischer, M. (2017). Census and evaluation of p53 target genes. *Oncogene*, *36*(28), 3943-3956.
983 https://doi.org/10.1038/onc.2016.502
984 Francis, M. J., Roche, S., Cho, M. J., Beall, E., Min, B., Panganiban, R. P., & Rio, D. C. (2016).
985 Drosophila IRBP bZIP heterodimer binds P-element DNA and affects hybrid dysgenesis.
986 *Proc Natl Acad Sci U S A*, *113*(46), 13003-13008.
987 https://doi.org/10.1073/pnas.1613508113
988 Freeman, M. (1996). Reiterative use of the EGF receptor triggers differentiation of all cell types
989 in the Drosophila eye. *Cell*, *87*(4), 651-660. https://doi.org/10.1016/s0092-
990 8674(00)81385-9
991 Hanks, S., Coleman, K., Reid, S., Plaja, A., Firth, H., Fitzpatrick, D., Kidd, A., Mehes, K., Nash, R.,
992 Robin, N., Shannon, N., Tolmie, J., Swansbury, J., Irrthum, A., Douglas, J., & Rahman, N.
993 (2004). Constitutional aneuploidy and cancer predisposition caused by biallelic
994 mutations in BUB1B. *Nat Genet*, *36*(11), 1159-1161. https://doi.org/ng1449 [pii]
995 10.1038/ng1449
996 Hopkins, J. L., Lan, L., & Zou, L. (2022). DNA repair defects in cancer and therapeutic
997 opportunities. *Genes Dev*, *36*(5-6), 278-293. https://doi.org/10.1101/gad.349431.122
998 Ji, Z., Chuen, J., Kiparaki, M., & Baker, N. (2021a). Cell competition removes segmental
999 aneuploid cells from Drosophila imaginal disc-derived tissues based on ribosomal
1000 protein gene dose. *Elife*, *10*, e61172. https://doi.org/10.7554/eLife.61172
1001 Ji, Z., Chuen, J., Kiparaki, M., & Baker, N. (2021b). Cell competition removes segmental
1002 aneuploid cells from Drosophila imaginal disc-derived tissues based on ribosomal
1003 protein gene dose. *Elife*, *10*. https://doi.org/10.7554/eLife.61172
1004 Ji, Z., Kiparaki, M., Folgado, V., Kumar, A., Blanco, J., Rimesso, G., Chuen, J., Liu, Y., Zheng, D., &
1005 Baker, N. E. (2019). Drosophila RpS12 controls translation, growth, and cell competition
1006 through Xrp1. *PLoS Genet*, *15*(12), e1008513.
1007 https://doi.org/10.1371/journal.pgen.1008513

1008 Jin, S., Martinek, S., Joo, W. S., Wortman, J. R., Mirkovic, N., Sali, A., Yandell, M. D., Pavletich, N.
1009 P., Young, M. W., & Levine, A. J. (2000). Identification and characterization of a p53
1010 homologue in Drosophila melanogaster. *Proc Natl Acad Sci U S A*, *97*(13), 7301-7306.
1011 https://doi.org/10.1073/pnas.97.13.7301
1012 Kaiser, A. M., & Attardi, L. D. (2018). Deconstructing networks of p53-mediated tumor
1013 suppression in vivo. *Cell Death Differ*, *25*(1), 93-103.
1014 https://doi.org/10.1038/cdd.2017.171
1015 Kakemura, B., Kanda, H., Matsumoto, R., Ueda, S., Yasuhara, S., Nagata, R., Taniguchi, K.,
1016 Kondo, S., Miyoshi, K., Kobayashi, T., Takeuchi, K., Saito, K., Matsuyama, M., Murakawa,
1017 Y., & Igaki, T. (2025). Cellular fitness is determined by ribosomal protein S12-1
1018 mediated release of a truncated Xrp1. *bioRxiv*, *preprint*.
1019 https://doi.org/https://doi.org/10.1101/2025.10.29.685279
1020 Kale, A., Ji, Z., Kiparaki, M., Blanco, J., Rimesso, G., Flibotte, S., & Baker, N. E. (2018). Ribosomal
1021 Protein S12e Has a Distinct Function in Cell Competition. *Dev Cell*, *44*(1), 42-55 e44.
1022 https://doi.org/10.1016/j.devcel.2017.12.007
1023 Kale, A., Li, W., Lee, C. H., & Baker, N. E. (2015). Apoptotic mechanisms during competition of
1024 ribosomal protein mutant cells: roles of the initiator caspases Dronc and Dream/Strica.
1025 *Cell Death Differ*, *22*(8), 1300-1312. https://doi.org/10.1038/cdd.2014.218
1026 Kastenhuber, E. R., & Lowe, S. W. (2017). Putting p53 in Context. *Cell*, *170*(6), 1062-1078.
1027 https://doi.org/10.1016/j.cell.2017.08.028
1028 Khan, C., Muliyil, S., Ayyub, C., & Rao, B. J. (2017). The initiator caspase Dronc plays a non-
1029 apoptotic role in promoting DNA damage signalling in D. melanogaster. *J Cell Sci*,
1030 *130*(18), 2984-2995. https://doi.org/10.1242/jcs.200782
1031 Khandekar, A., & Ellis, S. J. (2024). An expanded view of cell competition. *Development*, *151*(22).
1032 https://doi.org/10.1242/dev.204212
1033 Kiparaki, M., & Baker, N. E. (2023). Ribosomal protein mutations and cell competition:
1034 autonomous and nonautonomous effects on a stress response. *Genetics*, *224*(3).
1035 https://doi.org/10.1093/genetics/iyad080
1036 Kiparaki, M., Khan, C., Folgado-Marco, V., Chuen, J., Moulos, P., & Baker, N. E. (2022). The
1037 transcription factor Xrp1 orchestrates both reduced translation and cell competition
1038 upon defective ribosome assembly or function. *Elife*, *11*, e71705.
1039 https://doi.org/10.7554/eLife.71705
1040 Kucinski, I., Dinan, M., Kolahgar, G., & Piddini, E. (2017). Chronic activation of JNK JAK/STAT and
1041 oxidative stress signalling causes the loser cell status. *Nat Commun*, *8*(1), 136.
1042 https://doi.org/10.1038/s41467-017-00145-y
1043 Kumar, A., & Baker, N. E. (2022). The CRL4 E3 ligase Mahjong/DCAF1 controls cell competition
1044 through the transcription factor Xrp1, independently of polarity genes. *Development*,
1045 *149*(22). https://doi.org/10.1242/dev.200795
1046 Kurtz, P., Jones, A. E., Tiwari, B., Link, N., Wylie, A., Tracy, C., Kramer, H., & Abrams, J. M. (2019).
1047 Drosophila p53 directs nonapoptotic programs in postmitotic tissue. *Mol Biol Cell*,
1048 *30*(11), 1339-1351. https://doi.org/10.1091/mbc.E18-12-0791
1049 Lacroix, M., Riscal, R., Arena, G., Linares, L. K., & Le Cam, L. (2020). Metabolic functions of the
1050 tumor suppressor p53: Implications in normal physiology, metabolic disorders, and
1051 cancer. *Mol Metab*, *33*, 2-22. https://doi.org/10.1016/j.molmet.2019.10.002

1052 Lake, C. M., Holsclaw, J. K., Bellendir, S. P., Sekelsky, J., & Hawley, R. S. (2013). The development
1053 of a monoclonal antibody recognizing the Drosophila melanogaster phosphorylated
1054 histone H2A variant (gamma-H2AV). *G3 (Bethesda)*, *3*(9), 1539-1543.
1055 https://doi.org/10.1534/g3.113.006833
1056 Lee, C. H., Kiparaki, M., Blanco, J., Folgado, V., Ji, Z., Kumar, A., Rimesso, G., & Baker, N. E.
1057 (2018a). A Regulatory Response to Ribosomal Protein Mutations Controls Translation,
1058 Growth, and Cell Competition. *Dev Cell*, *46*(4), 456-469 e454.
1059 https://doi.org/10.1016/j.devcel.2018.07.003
1060 Lee, C. H., Kiparaki, M., Blanco, J., Folgado, V., Ji, Z., Kumar, A., Rimesso, G., & Baker, N. E.
1061 (2018b). A Regulatory Response to Ribosomal Protein Mutations Controls Translation,
1062 Growth, and Cell Competition. *Dev Cell*, *46*(6), 807.
1063 https://doi.org/10.1016/j.devcel.2018.09.009
1064 Lee, C. H., Rimesso, G., Reynolds, D. M., Cai, J., & Baker, N. E. (2016). Whole-Genome
1065 Sequencing and iPLEX MassARRAY Genotyping Map an EMS-Induced Mutation Affecting
1066 Cell Competition in Drosophila melanogaster. *G3 (Bethesda)*, *6*(10), 3207-3217.
1067 https://doi.org/10.1534/g3.116.029421
1068 Levine, A. J., Hu, W., & Feng, Z. (2006). The P53 pathway: what questions remain to be
1069 explored? *Cell Death Differ*, *13*(6), 1027-1036. https://doi.org/10.1038/sj.cdd.4401910
1070 Li, T., Kon, N., Jiang, L., Tan, M., Ludwig, T., Zhao, Y., Baer, R., & Gu, W. (2012). Tumor
1071 suppression in the absence of p53-mediated cell-cycle arrest, apoptosis, and
1072 senescence. *Cell*, *149*(6), 1269-1283. https://doi.org/10.1016/j.cell.2012.04.026
1073 Li, W., & Baker, N. E. (2007). Engulfment is required for cell competition. *Cell*, *129*(6), 1215-
1074 1225. https://doi.org/S0092-8674(07)00535-1 [pii]
1075 10.1016/j.cell.2007.03.054
1076 Li, Z., Wu, C., Ding, X., Li, W., & Xue, L. (2020). Toll signaling promotes JNK-dependent apoptosis
1077 in Drosophila. *Cell Div*, *15*, 7. https://doi.org/10.1186/s13008-020-00062-5
1078 Marusyk, A., Porter, C. C., Zaberezhnyy, V., & DeGregori, J. (2010). Irradiation selects for p53-
1079 deficient hematopoietic progenitors. *PLoS Biol*, *8*(3), e1000324.
1080 https://doi.org/10.1371/journal.pbio.1000324
1081 Marygold, S. J., Roote, J., Reuter, G., Lambertsson, A., Ashburner, M., Millburn, G. H., Harrison,
1082 P. M., Yu, Z., Kenmochi, N., Kaufman, T. C., Leevers, S. J., & Cook, K. R. (2007). The
1083 ribosomal protein genes and Minute loci of Drosophila melanogaster [Comparative
1084 Study
1085 Research Support, N.I.H., Extramural
1086 Research Support, Non-U.S. Gov't]. *Genome Biol*, *8*(10), R216. https://doi.org/10.1186/gb-2007-
1087 8-10-r216
1088 McNamee, L. M., & Brodsky, M. H. (2009). p53-independent apoptosis limits DNA damage-
1089 induced aneuploidy. *Genetics*, *182*(2), 423-435.
1090 https://doi.org/10.1534/genetics.109.102327
1091 genetics.109.102327 [pii]
1092 Morata, G., & Ripoll, P. (1975). Minutes: mutants of *Drosophila* autonomously affecting cell
1093 division rate. *Developmental Biology*, *42*, 211-221.
1094 Moreno, E., Basler, K., & Morata, G. (2002). Cells compete for decapentaplegic survival factor to
1095 prevent apoptosis in *Drosophila* wing development. *Nature*, *416*, 755-759.

1096 Muller, P. A., & Vousden, K. H. (2014). Mutant p53 in cancer: new functions and therapeutic
1097 opportunities. *Cancer Cell*, *25*(3), 304-317. https://doi.org/10.1016/j.ccr.2014.01.021
1098 Nagata, R., & Igaki, T. (2024). Cell competition: emerging signaling and unsolved questions.
1099 *FEBS Lett*, *598*(4), 379-389. https://doi.org/10.1002/1873-3468.14822
1100 Nemeth, E., & Szuts, D. (2024). The mutagenic consequences of defective DNA repair. *DNA*
1101 *Repair (Amst)*, *139*, 103694. https://doi.org/10.1016/j.dnarep.2024.103694
1102 Newsome, T. P., Asling, B., & Dickson, B. J. (2000). Analysis of Drosophila photoreceptor axon
1103 guidance in eye-specific mosaics. *Development*, *127*(4), 851-860.
1104 https://doi.org/10.1242/dev.127.4.851
1105 Ni, J. Q., Zhou, R., Czech, B., Liu, L. P., Holderbaum, L., Yang-Zhou, D., Shim, H. S., Tao, R.,
1106 Handler, D., Karpowicz, P., Binari, R., Booker, M., Brennecke, J., Perkins, L. A., Hannon,
1107 G. J., & Perrimon, N. (2011). A genome-scale shRNA resource for transgenic RNAi in
1108 Drosophila. *Nat Methods*, *8*(5), 405-407. https://doi.org/10.1038/nmeth.1592
1109 Ochi, N., Nakamura, M., Nagata, R., Wakasa, N., Nakano, R., & Igaki, T. (2021). Cell competition
1110 is driven by Xrp1-mediated phosphorylation of eukaryotic initiation factor 2alpha. *PLoS*
1111 *Genet*, *17*(12), e1009958. https://doi.org/10.1371/journal.pgen.1009958
1112 Ollmann, M., Young, L. M., Di Como, C. J., Karim, F., Belvin, M., Robertson, S., Whittaker, K.,
1113 Demsky, M., Fisher, W. W., Buchman, A., Duyk, G., Friedman, L., Prives, C., & Kopczynski,
1114 C. (2000). Drosophila p53 is a structural and functional homolog of the tumor
1115 suppressor p53 [Research Support, Non-U.S. Gov't
1116 Research Support, U.S. Gov't, P.H.S.]. *Cell*, *101*(1), 91-101. https://doi.org/10.1016/S0092-
1117 8674(00)80626-1
1118 Picco, V., & Pages, G. (2013). Linking JNK Activity to the DNA Damage Response. *Genes Cancer*,
1119 *4*(9-10), 360-368. https://doi.org/10.1177/1947601913486347
1120 Pilley, S., Rodriguez, T. A., & Vousden, K. H. (2021). Mutant p53 in cell-cell interactions. *Genes*
1121 *Dev*, *35*(7-8), 433-448. https://doi.org/10.1101/gad.347542.120
1122 Potiri, M., Tsakiri, E., Kontogiannidi, K., Loizou, M., Skoulakis, E. M. C., Samiotaki, M., Kafasla, P.,
1123 & Kiparaki, M. (2025). RPS12-mediated induction of the Xrp1-short isoform links
1124 ribosomal protein mutations to cell competition. *bioRxiv*,
1125 *https://doi.org/10.1101/2025.06.15.659587*.
1126 https://doi.org/https://doi.org/10.1101/2025.06.15.659587
1127 Recasens-Alvarez, C., Alexandre, C., Kirkpatrick, J., Nojima, H., Huels, D. J., Snijders, A. P., &
1128 Vincent, J. P. (2021). Ribosomopathy-associated mutations cause proteotoxic stress that
1129 is alleviated by TOR inhibition. *Nat Cell Biol*, *23*(2), 127-135.
1130 https://doi.org/10.1038/s41556-020-00626-1
1131 Reinke, A. W., Baek, J., Ashenberg, O., & Keating, A. E. (2013). Networks of bZIP protein-protein
1132 interactions diversified over a billion years of evolution. *Science*, *340*(6133), 730-734.
1133 https://doi.org/10.1126/science.1233465
1134 Riley, T., Sontag, E., Chen, P., & Levine, A. (2008). Transcriptional control of human p53-
1135 regulated genes. *Nat Rev Mol Cell Biol*, *9*(5), 402-412. https://doi.org/10.1038/nrm2395
1136 Rohr, C. O., Parra, R. G., Yankilevich, P., & Perez-Castro, C. (2013). INSECT: IN-silico SEarch for
1137 Co-occurring Transcription factors. *Bioinformatics*, *29*(22), 2852-2858.
1138 https://doi.org/10.1093/bioinformatics/btt506

1139 Ruiz-Losada, M., Gonzalez, R., Peropadre, A., Gil-Galvez, A., Tena, J. J., Baonza, A., & Estella, C.
1140 (2022). Coordination between cell proliferation and apoptosis after DNA damage in
1141 Drosophila. *Cell Death Differ*, *29*(4), 832-845. https://doi.org/10.1038/s41418-021-
1142 00898-6
1143 Sanchez, J. A., Mesquita, D., Ingaramo, M. C., Ariel, F., Milan, M., & Dekanty, A. (2019).
1144 Eiger/TNFalpha-mediated Dilp8 and ROS production coordinate intra-organ growth in
1145 Drosophila. *PLoS Genet*, *15*(8), e1008133.
1146 https://doi.org/10.1371/journal.pgen.1008133
1147 Shekhar, S., Tracy, C., Lidsky, P. V., Andino, R., Wert, K. J., & Kramer, H. (2025). Sensory
1148 quiescence induces a cell-non-autonomous integrated stress response curbed by
1149 condensate formation of the ATF4 and XRP1 effectors. *Nat Commun*, *16*(1), 252.
1150 https://doi.org/10.1038/s41467-024-55576-1
1151 Simpson, P. (1979). Parameters of cell competition in the compartments of the wing disc of
1152 *Drosophila*. *Developmental Biology*, *69*, 182-193.
1153 Singla, S., Iwamoto-Stohl, L. K., Zhu, M., & Zernicka-Goetz, M. (2020). Autophagy-mediated
1154 apoptosis eliminates aneuploid cells in a mouse model of chromosome mosaicism. *Nat*
1155 *Commun*, *11*(1), 2958. https://doi.org/10.1038/s41467-020-16796-3
1156 Spradling, A. C., Stern, D., Beaton, A., Rhem, E. J., Laverty, T., Mozden, N., Misra, S., & Rubin, G.
1157 M. (1999). The Berkeley Drosophila Genome Project gene disruption project: Single P-
1158 element insertions mutating 25% of vital Drosophila genes. *Genetics*, *153*(1), 135-177.
1159 https://doi.org/10.1093/genetics/153.1.135
1160 Struhl, G., & Basler, K. (1993). Organizing activity of wingless protein in Drosophila. *Cell*, *72*(4),
1161 527-540. https://doi.org/10.1016/0092-8674(93)90072-x
1162 Sykiotis, G. P., & Bohmann, D. (2008). Keap1/Nrf2 signaling regulates oxidative stress tolerance
1163 and lifespan in Drosophila. *Dev Cell*, *14*(1), 76-85.
1164 https://doi.org/10.1016/j.devcel.2007.12.002
1165 Tanaka-Matakatsu, M., Xu, J., Cheng, L., & Du, W. (2009). Regulation of apoptosis of rbf mutant
1166 cells during Drosophila development. *Dev Biol*, *326*(2), 347-356.
1167 https://doi.org/10.1016/j.ydbio.2008.11.035
1168 Titen, S. W., & Golic, K. G. (2008). Telomere loss provokes multiple pathways to apoptosis and
1169 produces genomic instability in Drosophila melanogaster. *Genetics*, *180*(4), 1821-1832.
1170 https://doi.org/10.1534/genetics.108.093625
1171 genetics.108.093625 [pii]
1172 Tiwari, V., & Wilson, D. M., 3rd. (2019). DNA Damage and Associated DNA Repair Defects in
1173 Disease and Premature Aging. *Am J Hum Genet*, *105*(2), 237-257.
1174 https://doi.org/10.1016/j.ajhg.2019.06.005
1175 Tsurui-Nishimura, N., Nguyen, T. Q., Katsuyama, T., Minami, T., Furuhashi, H., Oshima, Y., &
1176 Kurata, S. (2013). Ectopic antenna induction by overexpression of CG17836/Xrp1
1177 encoding an AT-hook DNA binding motif protein in Drosophila [Research Support, Non-
1178 U.S. Gov't]. *Biosci Biotechnol Biochem*, *77*(2), 339-344.
1179 https://doi.org/10.1271/bbb.120756
1180 Vijg, J. (2021). From DNA damage to mutations: All roads lead to aging. *Ageing Res Rev*, *68*,
1181 101316. https://doi.org/10.1016/j.arr.2021.101316

1182 Vincent, J. P., Girdham, C. H., & O'Farrell, P. H. (1994). A cell-autonomous, ubiquitous marker
1183 for the analysis of Drosophila genetic mosaics. *Dev Biol*, *164*(1), 328-331.
1184 https://doi.org/10.1006/dbio.1994.1203
1185 Wagstaff, L., Goschorska, M., Kozyrska, K., Duclos, G., Kucinski, I., Chessel, A., Hampton-O'Neil,
1186 L., Bradshaw, C. R., Allen, G. E., Rawlins, E. L., Silberzan, P., Carazo Salas, R. E., & Piddini,
1187 E. (2016). Mechanical cell competition kills cells via induction of lethal p53 levels. *Nat*
1188 *Commun*, *7*, 11373. https://doi.org/10.1038/ncomms11373
1189 Wei, C. L., Wu, Q., Vega, V. B., Chiu, K. P., Ng, P., Zhang, T., Shahab, A., Yong, H. C., Fu, Y., Weng,
1190 Z., Liu, J., Zhao, X. D., Chew, J. L., Lee, Y. L., Kuznetsov, V. A., Sung, W. K., Miller, L. D.,
1191 Lim, B., Liu, E. T.,…Ruan, Y. (2006). A global map of p53 transcription-factor binding sites
1192 in the human genome. *Cell*, *124*(1), 207-219. https://doi.org/10.1016/j.cell.2005.10.043
1193 Wells, B. S., Yoshida, E., & Johnston, L. A. (2006). Compensatory proliferation in Drosophila
1194 imaginal discs requires Dronc-dependent p53 activity. *Curr Biol*, *16*(16), 1606-1615.
1195 https://doi.org/10.1016/j.cub.2006.07.046
1196 Wichmann, A., Jaklevic, B., & Su, T. T. (2006). Ionizing radiation induces caspase-dependent but
1197 Chk2- and p53-independent cell death in Drosophila melanogaster. *Proc Natl Acad Sci U*
1198 *S A*, *103*(26), 9952-9957. https://doi.org/10.1073/pnas.0510528103
1199 Wichmann, A., Uyetake, L., & Su, T. T. (2010). E2F1 and E2F2 have opposite effects on radiation-
1200 induced p53-independent apoptosis in Drosophila. *Dev Biol*, *346*(1), 80-89.
1201 https://doi.org/10.1016/j.ydbio.2010.07.023
1202 Williams, A. B., & Schumacher, B. (2016). p53 in the DNA-Damage-Repair Process. *Cold Spring*
1203 *Harb Perspect Med*, *6*(5). https://doi.org/10.1101/cshperspect.a026070
1204 Xu, T., & Rubin, G. M. (1993). Analysis of genetic mosaics in developing and adult Drosophila
1205 tissues. *Development*, *117*(4), 1223-1237. https://doi.org/10.1242/dev.117.4.1223
1206 Zhang, B., Mehrotra, S., Ng, W. L., & Calvi, B. R. (2014). Low levels of p53 protein and chromatin
1207 silencing of p53 target genes repress apoptosis in Drosophila endocycling cells. *PLoS*
1208 *Genet*, *10*(9), e1004581. https://doi.org/10.1371/journal.pgen.1004581
1209 Zhang, G., Xie, Y., Zhou, Y., Xiang, C., Chen, L., Zhang, C., Hou, X., Chen, J., Zong, H., & Liu, G.
1210 (2017). p53 pathway is involved in cell competition during mouse embryogenesis. *Proc*
1211 *Natl Acad Sci U S A*, *114*(3), 498-503. https://doi.org/10.1073/pnas.1617414114
1212 Zhang, X. P., Liu, F., & Wang, W. (2011). Two-phase dynamics of p53 in the DNA damage
1213 response. *Proc Natl Acad Sci U S A*, *108*(22), 8990-8995.
1214 https://doi.org/10.1073/pnas.1100600108
1215 Zhu, L. J., Christensen, R. G., Kazemian, M., Hull, C. J., Enuameh, M. S., Basciotta, M. D.,
1216 Brasefield, J. A., Zhu, C., Asriyan, Y., Lapointe, D. S., Sinha, S., Wolfe, S. A., & Brodsky, M.
1217 H. (2011). FlyFactorSurvey: a database of Drosophila transcription factor binding
1218 specificities determined using the bacterial one-hybrid system. *Nucleic Acids Res*,
1219 *39*(Database issue), D111-117. https://doi.org/10.1093/nar/gkq858
1220